Evaluation of a Series of Naphthamides as Potent, Orally Active Vascular Endothelial Growth Factor Receptor-2 Tyrosine Kinase Inhibitors[¶]

Matthew M. Weiss,*[,†] Jean-Christophe Harmange,[†] Anthony J. Polverino,[‡] David Bauer,[†] Loren Berry,[#] Virginia Berry,[#] George Borg,[†] James Bready,[‡] Danlin Chen,[‡] Deborah Choquette,[†] Angela Coxon,[‡] Tom DeMelfi,[‡] Nicholas Doerr,[‡] Juan Estrada,[‡] Julie Flynn,[#] Russell F. Graceffa,[†] Shawn P. Harriman,[#] Stephen Kaufman,[||] Daniel S. La,[†] Alexander Long,[§] Sesha Neervannan,[×,∞] Vinod F. Patel,[†] Michele Potashman,[†] Kelly Regal,[#] Phillip M. Roveto,[†] Michael L. Schrag,[#] Charlie Starnes,[‡] Andrew Tasker,[†] Yohannes Teffera,[#] Douglas A. Whittington,[§] and Roger Zanon[×]

Department of Medicinal Chemistry, Department of Molecular Structure, and Department of Pharmacokinetics and Drug Metabolism, Amgen Inc., One Kendall Square, Building 1000, Cambridge, Massachusetts 02139, and Department of Oncology Research, Department of Toxicology, and Department of Pharmaceutics, Amgen Inc., One Amgen Center Drive, Thousand Oaks, California 91320

Received September 4, 2007

We have previously shown *N*-arylnaphthamides can be potent inhibitors of vascular endothelial growth factor receptors (VEGFRs). *N*-Alkyl and *N*-unsubstituted naphthamides were prepared and found to yield nanomolar inhibitors of VEGFR-2 (KDR) with an improved selectivity profile against a panel of tyrosine and serine/threonine kinases. The inhibitory activity of this series was retained at the cellular level. Naphthamides **3**, **20**, and **22** exhibited good pharmacokinetics following oral dosing and showed potent inhibition of VEGF-induced angiogenesis in the rat corneal model. Once-daily oral administration of **22** for 14 days led to 85% inhibition of established HT29 colon cancer and Calu-6 lung cancer xenografts at doses of 10 and 20 mg/kg, respectively.

Angiogenesis is of importance to many normal physiological processes but also contributes to pathological disorders and, in particular, has implications in the growth and metastasis of solid tumors.[1,2] Tumors smaller than 2 mm^3 in volume acquire nutrients and oxygen via passive diffusion; however, in order for growth beyond this critical size, an increase in vasculature is required.[3] Neovascularization results from a complex set of events involving a number of diverse stimuli; however, signaling induced by VEGF[a] is considered rate-limiting. VEGF drives the angiogenic cascade by promoting endothelial cell activation and proliferation and enhancing the migration and invasion of endothelial cells. Tumors can up-regulate VEGF expression or secretion via a number of pathways, including oncogene activation,[4] loss of tumor suppressor function,[5] and changes in oxygen levels.[6] VEGF binds to the receptor tyrosine kinase (RTK) receptors including VEGFR-2 (KDR) on endothelial cells, which initiates a dimerization event.[7,8] The resulting conformational change induced in the receptor complex leads to the propagation of intracellular signaling cascades that result in altered gene expression and cellular function.

Inhibition of angiogenesis by blocking the VEGF signaling pathway has attracted considerable interest as an approach to anticancer therapy.[9]Indeed, this approach has recently been validated with the VEGF monoclonal antibody bevacizumab, which has been approved by the FDA for the treatment of metastatic colorectal cancer and non-small-cell lung cancer.[10] In addition to biological-based antiangiogenics, many small-molecule KDR inhibitors are currently in clinical development[11–13] and two inhibitors, sorafenib[14] and sunitinib,[15] have recently received approval for the treatment of renal cell carcinoma. Our program has targeted the development of small-molecule inhibitors of KDR, such as AMG 706 (*N*-(3,3-dimethyl-2,3-dihydro-1*H*-indol-6-yl)-2-(pyridin-4-ylmethylamino)pyridine-3-carboxamide, motesanib diphosphate).[16] This compound was recently reported as a highly selective oral agent that is being evaluated for its ability to inhibit angiogenesis and lymphangiogenesis by targeting vascular endothelial growth factor receptors (VEGFR) 1–3.[16] It is also under investigation for its potential direct antitumor activity by targeting platelet-derived growth factor receptor (PDGFR) and stem cell factor receptor (c-Kit) signaling. Motesanib diphosphate is currently in phase 2 development as a monotherapy in thyroid cancer and in combination with other anticancer therapies to treat patients with non-small-cell lung cancer, breast cancer, and colorectal cancer.

In the previous Article, we reported the design, synthesis, and evaluation of a series of *N*-arylnaphthamides (**1**, Figure 1).[18] This scaffold provided access to low-nanomolar inhibitors of KDR and led to the identification of **2** (Figure 1), which demonstrated robust preclinical in vivo activity in a human tumor xenograft model. While efficacious in several in vivo models, this agent lacked a high degree of selectivity against several kinases. Of particular concern was inhibitory activity against the serine/threonine kinase (STK) Aurora B, a mitotic kinase that has been implicated in centrosome separation and spindle formation,[19] and the nonreceptor tyrosine kinase (NRTK)

[¶] The PDB accession codes for cocrystals of compounds **2** and **3** in the KDR ATP-binding pocket are 3B8Q and 3B8R, respectively.

* To whom correspondence should be addressed. Phone: 617-444-5188. Fax: 617-621-3908. E-mail: mmweiss@amgen.com.

[†] Department of Medicinal Chemistry.

[‡] Department of Oncology Research.

[#] Department of Pharmacokinetics and Drug Metabolism.

[||] Department of Pathology.

[§] Department of Molecular Structure.

[×] Department of Pharmaceutics.

[∞] Present Address: Allergan, 2525 Dupont Drive, Irvine, CA 92623.

[a] Abbreviations: VEGF, vascular endothelial growth factor; KDR, kinase domain region; PDGFR, platelet-derived growth factor receptor; HUVEC, human umbilical vein endothelial cells; STK, serine/threonine kinase; NRTK, nonreceptor tyrosine kinase; bFGF, basic fibroblast growth factor; FBS, fetal bovine serum; PBS, phosphate buffered saline; MRT, mean residence time; DMF, dimethylformamide; DMSO, dimethyl sulfoxide; DIPEA, diisopropylethylamine; DMAP, 4-dimethylaminopyridine; HATU, 2-(7-aza-1*H*-benzotriazole-1-yl)-1,1,3,3-tetramethyluronium hexafluorophosphate; HOAt, 1-hydroxy-7-azabenzotriazole; EDC, *N*-ethyl-*N*′-(3-dimethylaminopropyl)carbodiimide hydrochloride; MSA, methanesulfonic acid.

10.1021/jm701098w CCC: $40.75
Published on Web 03/07/2008

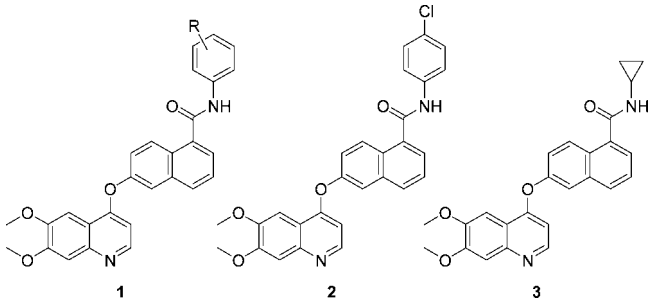

Figure 1. Lead Discovery for *N*-alkylnaphthamides.

Table 1. Selectivity Profiles for **2** and **3**

	IC_{50}[a] (nM)						
compd	KDR	Tie-2	c-Met	Lck	Aurora A	Aurora B	cLogP[b]
2	0.48	580	450	38	371	18	7.02
3	0.60	25000	20000	330	2000	118	4.61

[a] IC_{50} values were averaged values determined by at least two independent experiments. [b] Determined using Daylight software, version 4.41.[17]

Lck, a member of the Src family that has been shown to have important roles in T cell receptor signal transduction.[20] Furthermore, **2** possessed poor intrinsic physicochemical properties that included low aqueous solubility and high lipophilicity, as determined by cLogP (7.02).[17] These features led to restricted cell permeability, which in turn limited inhibition at the cellular level.

In the course of identifying **2**, it was found that *N*-cyclopropylnaphthamide **3** (Figure 1) was a potent inhibitor of KDR and displayed a more restrictive selectivity profile against a small panel of kinases (Table 1). In addition to improved selectivity, the reduced cLogP of **3** was expected to translate into improved cellular permeability and a more favorable pharmacokinetic profile.

In an effort to gain insight into the origin of the improved selectivity profile of **3**, we turned to the crystallographic structures of **2**[18] and **3** within the catalytic domain of KDR. As illustrated in Figure 2, both inhibitors bind to the enzyme in a similar manner, wherein the nitrogen of the dimethoxyquinoline ring participates in a hydrogen-bond interaction with the backbone amide-NH of Cys919 of the hinge region. The naphthyl core, which is oriented orthogonal to the quinoline ring, is accommodated in the mostly hydrophobic ATP-binding cleft. The carbonyl and NH groups of the amide make two interactions with the backbone NH of Asp1046 and the side chain of Glu885, respectively. Inspection of the two crystallographic structures, however, reveals a large conformational change in the highly conserved Asp-Phe-Gly (DFG) loop. When complexed with **2** (Figure 2), KDR adopts an "inactive" kinase conformation and the DFG loop of KDR assumes a "DFG-out" conformation, allowing the *p*-Cl phenyl ring of **2** to penetrate into the extended hydrophobic pocket which exists between the N- and C-terminal regions (PDB accession code 3B8Q). This conformational change, wherein Phe1047 has shifted by about 10 Å, opens up this extended hydrophobic pocket which cannot be accessed when the enzyme is in the "active" conformation. In contrast, when complexed with **3** (Figure 2), the DFG loop is maintained in a "DFG-in" conformation, preventing interactions between the inhibitor and the extended hydrophobic pocket (PDB accession code 3B8R). Interestingly, while **3** is not able to leverage interactions in the extended hydrophobic pocket, it maintained the potent level of inhibition exhibited by **2**. Herein, we describe the structure–activity

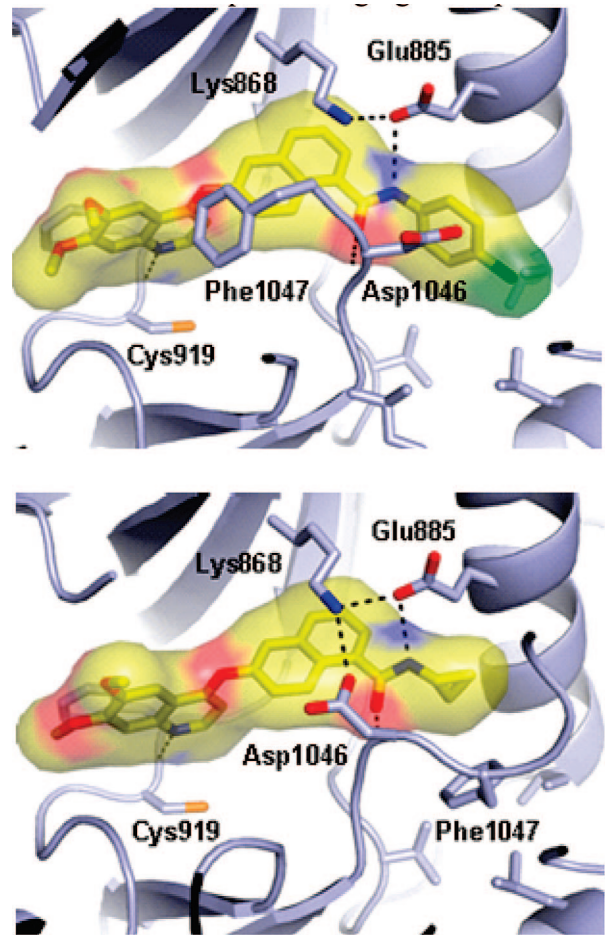

Figure 2. Crystallographic analysis of compounds **2** (top) and **3** (bottom) in the ATP-binding pocket of KDR. Hydrogen bonds are shown between the inhibitors and KDR (dotted lines).

relationships and antitumor activity of *N*-alkyl and *N*-unsubstituted naphthamides.[21]

Chemistry

The compounds described in Tables 2−3 were prepared by the general routes described in Scheme 1.[21] Commercially available 6-hydroxynaphthoic acid (**4**) was heated in the presence of cesium carbonate and the appropriately substituted 4-chloroquinoline[22] in DMSO to provide naphthoic acids **5a–c**. The naphthamides of interest (**6**) were then accessed via conversion of the acid to the desired amide functionality. Alternatively, 6-hydroxynaphthoic acid (**4**) could be converted to naphthamide **7**, which could then be transformed to the desired naphthamide (**6**) utilizing a modified Ullman procedure.[23] Compounds wherein the 6,7-dimethoxyquinoline was replaced with a 6,7-dimethoxyquinazoline (i.e., **9**) could be accessed in a similar manner. To this end, coupling of 6-hydroxynapthoic acid (**4**) with 4-chloro-6,7-dimethoxyquinazoline[24] in the presence of cesium carbonate provided naphthoic acid **8**, which could subsequently be elaborated to the desired naphthamides of interest.

Results and Discussion

To evaluate the aforementioned hypothesis that the improved selectivity profile of **3** was a result of the inhibitor binding the enzyme in a "DFG-in" conformation, a number of *N*-alkyl substituted and *N*-unsubstituted naphthamides were prepared. It was anticipated that inhibitors containing sterically unencum-

Table 2. Structure–Activity Relationship (SAR): Variations of the Naphthamide

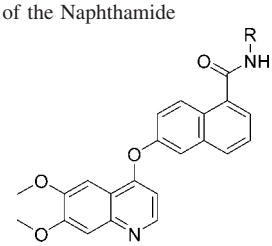

Cpd	R	IC_{50}[a] (nM)								
		KDR	Tie-2	c-Met	Lck	Aurora A	Aurora B	HUVEC[b] (VEGF)	HUVEC[b] (bFGF)	cLogP[c]
2		0.48	580	450	38	371	18	7.6	1140	7.02
3		0.60	25000	20000	330	2000	118	0.91	170	4.61
10		1.3	4000	7600	1000	440	ND	6.8	1140	5.17
11		15	1400	3200	1300	620	ND	6.6	1140	5.73
12		15	1100	5000	2000	560	62	70	1140	5.13
13		11	9400	5300	1100	840	10	22	1140	5.23
14		3.8	25000	20000	700	3600	110	0.45	46	4.25
15		1.3	25000	20000	1200	1500	46	0.33	150	4.78
16		1.3	4300	ND	1300	1700	ND	7.4	600	5.31
17		5.9	25000	20000	1800	3600	190	4.4	1140	5.09
18		1500	25000	11000	4300	3700	ND	ND	ND	5.49
19		3.8	25000	20000	25000	930	16	24	1140	5.54
20		12	25000	20000	1200	7200	130	0.64	1140	4.32
21		4.2	8300	ND	1000	3500	ND	7.1	1140	4.63
22		0.90	25000	6900	300	5000	220	2.1	230	4.05

[a] IC_{50} values were averaged values determined by at least two independent experiments. ND: Not Determined. [b] Human umbilical vein endothelial cells. [c] Determined using Daylight software, version 4.41.[17]

bered amides would bind KDR in a similar conformation as **3**. On the basis of previous work, initial structure–activity relationship (SAR) studies were investigated utilizing the 6,7-dimethoxyquinoline as the linker binding element. In addition to screening the naphthamides against a series of subfamilies of RTKs, including Tie-2 and c-Met, they were also screened against the NRTK Lck as well as the STKs Aurora A and B. Potency at the cellular level was evaluated by determining the inhibition of human umbilical vein endothelial cell (HUVEC) proliferation induced by either VEGF or basic fibroblast growth factor (bFGF). The cellular assay was carried out in the presence of 10% fetal bovine serum (FBS).

Inhibitors wherein the amide was either unsubstituted or substituted with small alkyl groups were generally well tolerated (Table 2). To this end, potent KDR inhibitors could be generated by incorporation of a linear alkyl group (**14**–**16**, **19**–**21**), a cycloalkyl group (**3**, **10**–**12**) or a branched alkyl group (**13**, **17**). The cyclopropylamide **3** and the free carboxamide **22** delivered the most KDR enzymatic potency, while cycloalkylamides **11** and **12** were slightly less potent and *tert*-butylamide **18** was not tolerated and exhibited drastically diminished potency. As eluded to previously, **3** demonstrated an improved selectivity profile when compared to naphthamide **2**. With the exception of Aurora B and Lck, the selectivity profile exhibited by **3** was well maintained within the series. The only compounds tested that were less than 400-fold selective for KDR over Tie-2 and c-Met were **11**, **12**, and **18**. Selectivity against Lck was less general; linear alkylamides **15**, **16**, and **19** as well as the small cycloalkylamides **3** and **10** demonstrated the highest degree of selectivity against Lck. With respect to Aurora B, compounds **12**, **13**, and **19** exhibited potent inhibition and were less than 6-fold selective for KDR over Aurora B.

The kinase inhibitory activity of these compounds generally translated well into the inhibition of growth factor-dependent cell proliferation. With the exception of three compounds (**12**, **13**, and **19**) all of the compounds tested exhibited single-digit nanomolar inhibition of VEGF-driven HUVEC proliferation. The high lipophilicity of **2** led to limited cellular permeability, and this manifested itself in a relatively large shift (>15) between the enzymatic assay and the cellular VEGF-driven HUVEC proliferation assay. Carboxamide **22** and most of the *N*-alkylnaphthamides illustrated in Table 2 are considerably less lipophilic than **2** and in turn exhibited a smaller shift between the enzymatic and cellular based assays. Furthermore, with the

Table 3. SAR: Variations of the Quinoline Linker Binding Element

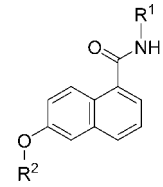

Compound	R^1	R^2	IC_{50}[a] (nM) KDR	Tie-2	c-Met	Aurora A	Aurora B	HUVEC[b] (VEGF)
23			2.9	7400	20000	8300	360	7.3
24		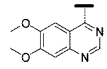	314	8300	20000	25000	385	ND
25			1.3	8300	20000	8300	680	16
26			0.45	8300	20000	8300	ND	3.4
27		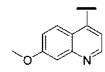	28	25000	20000	8300	ND	20
28			1.2	25000	20000	8300	130	16
29			0.37	1800	20000	4400	185	1.2
30		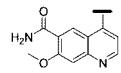	22	8300	6700	8300	233	0.80
31			1.3	5300	7400	6800	390	1.3

[a] IC_{50} values were averaged values determined by at least two independent experiments. ND: not determined. [b] Human umbilical vein endothelial cells.

Scheme 1. Preparation of Naphthamides[a]

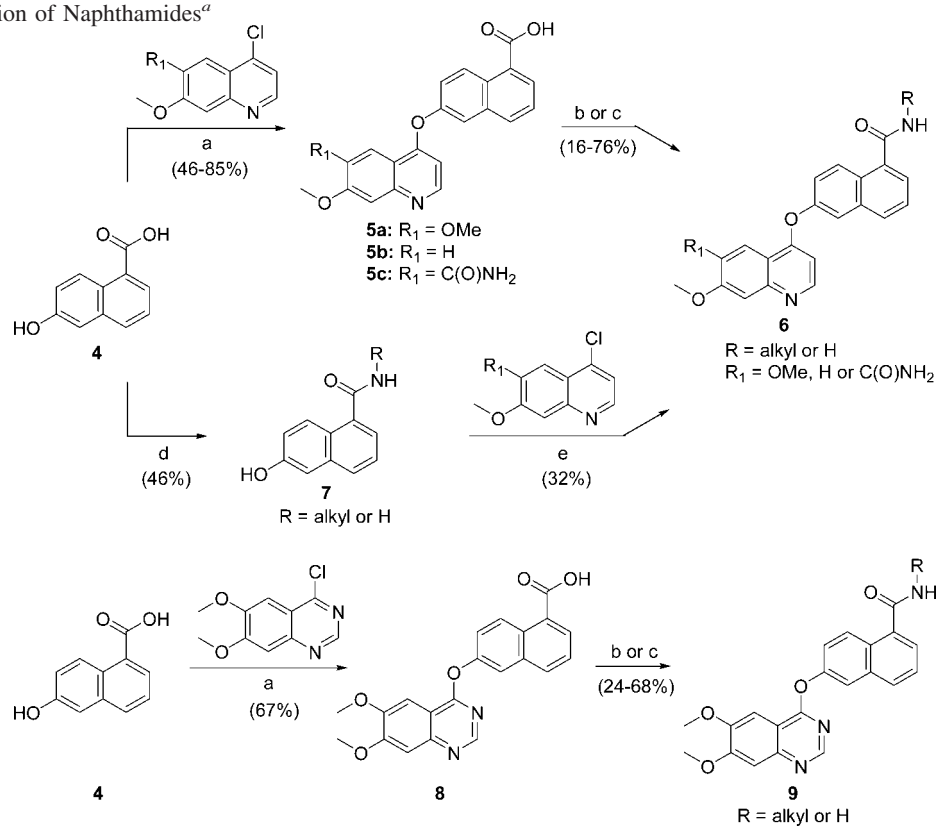

[a] Reagents: (a) Cs_2CO_3, DMSO, 140 °C; (b) $SOCl_2$, benzene, 65 °C; base, RNH_2, CH_2Cl_2; or oxalyl chloride, DMF, CH_2Cl_2; base, RNH_2, CH_2Cl_2; (c) HATU, DIPEA, RNH_2, CH_2Cl_2; (d) EDC, DIPEA, RNH_2 DMF; or HOAt, DIPEA, RNH_2, CH_2Cl_2; (e) Cu, KOH, pyridine, DMF 120 °C, microwave.

exception of **12**, **13**, **16**, and **19**, all the compounds tested showed preferential inhibition (>100-fold) of VEGF-dependent HUVEC proliferation when compared to their inhibition of bFGF-dependent proliferation.

Table 4. Metabolic Stability and Pharmacokinetic Parameters in Male Sprague–Dawley Rats

compd	metabolic stability RLM/HLM[a] ((μL/min)/mg)		iv Cl (mL/h·kg)	iv V_{ss} (mL/kg)	iv $t_{1/2}$ (h)	po $AUC_{0-\infty}$ (ng·h/mL)	po C_{max} (ng/mL)	po t_{max} (h)	po F (%)
3	21	31	131[b]	1038	8.4	50228[d]	6152	2.5	66
20	48	32	532[b]	1133	1.6	3771[e]	543	2.0	99
22	32	7	224[c]	1065	6.0	8450[e]	1689	1.6	96
29	16	12	508[c]	379	1.26	900[e]	715	0.67	39
30	95	4	3048[c]	751	0.31	164[e]	61	0.30	12

[a] Rat liver microsomal (RLM) and human liver microsomal (HLM) clearance. Compound concentration = 1 μM. Microsomal protein concentration = 1 mg/mL. [b] Dosed iv at 1 mg/kg as a solution in DMSO. [c] Dosed iv at 0.5 mg/kg as a solution in DMSO. [d] Dosed po at 10 mg/kg as a suspension in 100% OraPlus. [e] Dosed po at 2 mg/kg as a suspension in 100% OraPlus.

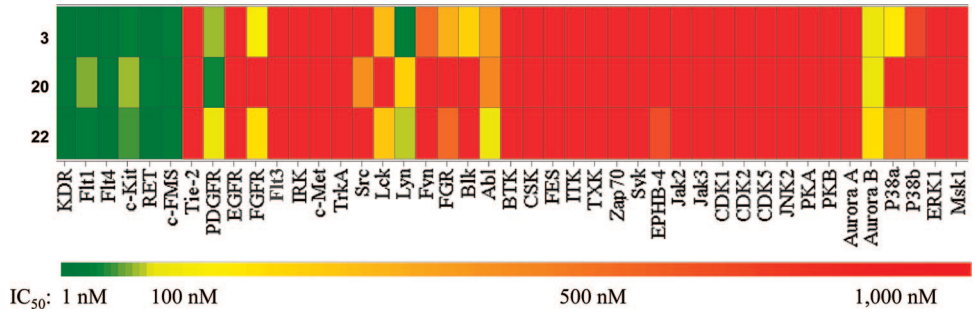

Figure 3. Kinase selectivity profile for **3**, **20**, and **22**.

The improved physicochemical properties of the *N*-alkyl and *N*-unsubstituted naphthamides relative to **2** also manifest themselves in improved aqueous solubility. Compounds **3**, **20**, and **22** were considerably more soluble in 0.01 N HCl (>200 μg/mL) than *N*-arylnaphthamide **2** (1.1 μg/mL).[25]

Replacement of the dimethoxyquinoline nucleus was also investigated (Table 3). In general, modifications to this region of the molecule led to inhibitors that maintained a good selectivity profile but decreased potency in the VEGF-driven HUVEC assay. This trend is exemplified in Table 3 wherein replacement of the 6,7-dimethoxyquinoline with 6,7-dimethoxyquinazoline and 7-methoxyquinoline resulted in inhibitors with diminished cellular potency. The exception to this trend were compounds containing the 7-methoxy-6-carboxamide quinoline core (**29**−**31**), which displayed similar potency to the respective compounds in the parent 6,7-dimethoxyquinoline series. This series of compounds maintained the moderate level of selectivity over Aurora B that was displayed by the 6,7-dimethoxyquinoline series.

In Vitro Metabolic Stability and Pharmacokinetic Profiles. On the basis of their in vitro potencies, the metabolic stability and pharmacokinetic profiles of several inhibitors were evaluated. Illustrated in Table 4 are the in vitro stabilities and pharmacokinetic profiles following intravenous (iv) and oral (po) dosing in male Sprague–Dawley rats. With the exception of **30**, all of the compounds examined demonstrated acceptable metabolic stability in rat liver microsomes (RLM $CL_{in\ vitro}$ < 50 (μL/min)/mg) and in turn exhibited low iv clearance (CL ≤ 600 mL/(h·kg)). Compound **30**, which demonstrated a higher rate of clearance in vitro (RLM $CL_{in\ vitro}$ = 95 (μL/min)/mg), was cleared at a high rate (3,048 mL/(h·kg)) and in turn displayed a shorter plasma-elimination half-life (0.30 h). After oral dosing the compounds in the 6,7-dimethoxyquinoline series (**3**, **20**, and **22**) all demonstrated good bioavailability and exposure levels with a t_{max} in the range 1.6–2.5 h. In contrast, compounds **29** and **30** were less bioavailable and consequently exhibited diminished levels of exposure.

Kinase Selectivity Profile. The inhibitory profiles of compounds **3**, **20**, and **22** were determined in a panel of in vitro kinase enzymes. As illustrated in the form of a heat map in Figure 3, the selectivity profiles for these compounds were similar among the kinases that were examined. Each compound demonstrated broad activity against the human VEGFR family (Flt-1/VEGFR1 and Flt-4/VEGFR3), with **20** being slightly less potent against Flt-1 (73 nM). Comparable levels of inhibitory activity were observed for the VEGFR and structurally related platelet-derived growth factor receptor (PDGFR) family of kinases. In this regard, all three compounds exhibited potent inhibition of c-Kit, c-fms, and PDGFRα; however, no inhibition of Flt-3 was observed. This selectivity is likely due to a disparity in the gatekeeper residue present in each of these kinases. This residue influences the accessibility of the hydrophobic pocket that flanks the ATP binding site, and its size can be a key factor in controlling kinase selectivity. In KDR this residue is a valine, while in c-Kit, c-fms, and PDGFRα it is a threonine. However, the gatekeeper residue in Flt-3 is a phenylalanine (Phe691). The compounds were highly selective against a broad range of other unrelated kinases tested, including EGFR, Src, and p38 kinase. As a whole, the compounds showed lower levels of selectivity for Abl and members of the Src-B family, including Lyn and FGR. Compound **3** has moderate potency for Abl (IC_{50} = 466 nM) and FGR (IC_{50} = 396 nM) and showed strong inhibition toward Lyn (IC_{50} = 27 nM). Compound **20** has a slightly improved selectivity profile and showed only modest potency against Lyn (IC_{50} = 275 nM). Compound **22** displayed moderate potency against both Lyn (IC_{50} = 88 nM) and Abl (IC_{50} = 110 nM).

Table 5. Inhibition of VEGF-Induced Vascular Permeability[a]

compd	active dose[b] (mg/kg)	concentration at active dose (μM)[c]
3	10	1.0
20	3	0.2
22	30	2.3

[a] n = 5 animals per group. [b] Dosed as a suspension in OraPlus. [c] Plasma concentration at t = 6 h.

In Vivo Inhibition of Vascular Permeability and Rat Corneal Angiogenesis. To confirm the results observed in the enzymatic assay and the VEGF-promoted HUVEC assay, the effects of **3**, **20**, and **22** were examined in a VEGF-induced

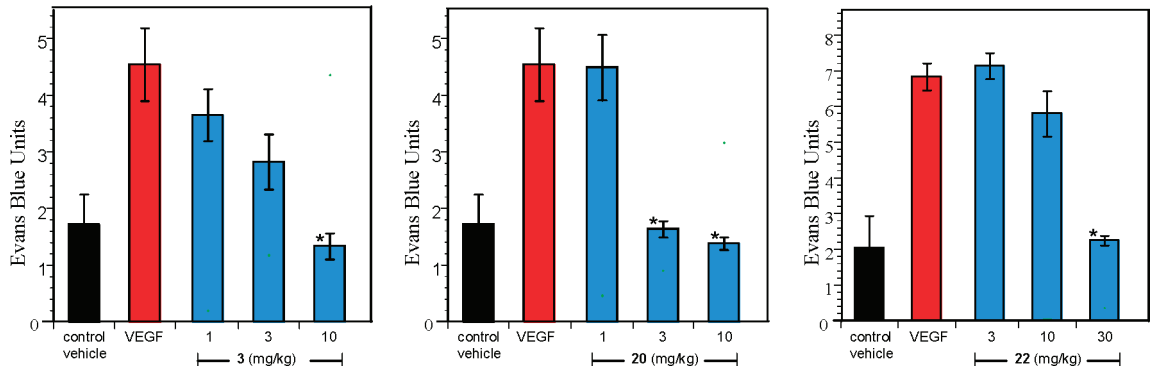

Figure 4. Effect of compounds **3**, **20**, and **22** on VEGF induced vascular permeability in mice ($n = 5$ animals per group). HEK 293 cells transfected with murine VEGF or vector were mixed with Matrigel and injected sc into CD-1 nu/nu mice. A single dose of compound was given and vascular permeability in the skin overlying the Matrigel plug assessed 6 h later. Data represent the mean ± standard error: (∗) $P \leq 0.0002$.

Table 6. Inhibition of VEGF-Induced Angiogenesis in Rats[a]

compd	ED_{50}[b] (mg/kg)	C_{max} (μM)	AUC_{0-24} (μM·h)
3	0.01	0.02	0.32
20	0.04	0.04	0.52
22	0.04	0.05	0.48

[a] $n = 8$ animals per group. [b] Dosed as a suspension in OraPlus.

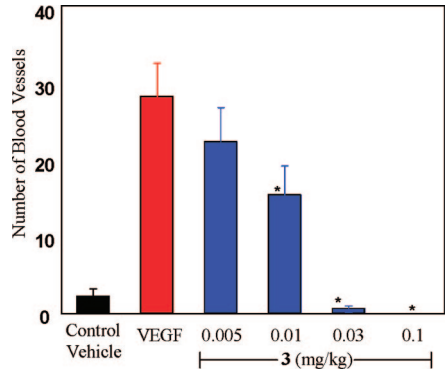

Figure 5. Inhibition of VEGF-induced angiogenesis in the rat cornea by **3**. Angiogenesis was induced by implanting a VEGF-soaked or BSA-soaked (control) nylon disk into the corneal stroma. The number of blood vessels intersecting the midpoint between the disk and the limbus was measured after 7 days of dosing vehicle or drug. Data represent the mean ± standard error ($n = 8$ animals per group): (∗) $P < 0.005$.

vascular permeability assay and a rat corneal angiogenesis model. In the vascular permeability model, HEK293 cells overexpressing recombinant murine VEGF were cultured, suspended in Matrigel, and injected subcutaneously (sc) onto the ventral surface of CD-1 nu/nu mice.[16] Twenty four hours after implantation, mice were dosed by oral gavage with either drug or vehicle. Six hours after administration of compound, vascular permeability was assessed by quantitation of Evans blue dye in a 1 cm^2 piece of skin overlying the Matrigel plug. As illustrated in Table 5 and Figure 4, compounds **3**, **20**, and **22** significantly inhibited vascular permeability at doses of 10, 3, and 30 mg/kg, respectively.

To evaluate the antiangiogenic activity of **3**, **20**, and **22** in vivo, these compounds were examined in a rat corneal angiogenesis model (Table 6).[16] Disks soaked with VEGF (10 μmol/L or BSA as a control) were implanted into a pocket in the corneal stroma of adult female Sprague–Dawley rats. The animals were dosed once daily (qd) with drug or vehicle. Following 7 days of treatment, the corneas were photographed and the number of vessels intersecting the midpoint between the disk and the limbus was measured. All three compounds inhibited VEGF-induced angiogenesis in a dose-responsive fashion, with the lowest ED_{50} (0.01 mg/kg) being achieved with **3** (Figure 5). Compounds **20** and **22** each displayed an ED_{50} of 0.04 mg/kg (Table 6).

While the efficacy and initial pharmacokinetic screening of **3** was promising, the presence of the cyclopropylamide was of some concern. It has been demonstrated that cyclopropylamines have a propensity to undergo P450-mediated bioactivation to electrophilic and/or free radical intermediates capable of covalently reacting with biomacromolecules and inducing a toxicological response.[26] It is generally recognized that covalent binding of reactive intermediates to proteins is an initial and crucial event in the etiology of many chemical-induced toxicities.[27] Hence, before evaluating **3** in an in vivo tumor growth setting, we evaluated ^{14}C-labeled **3** for the formation of reactive metabolites in the presence of rat and human liver microsomes.[28] Incubation of ^{14}C-labeled **3** with human liver microsomes led to moderate levels of covalent binding (357 (pmol/mg)/h) in an NADPH-dependent manner, indicating that metabolic activation was occurring (Table 7). Furthermore, the addition of glutathione (GSH) as an exogenous trapping agent in the microsomal incubation led to an approximate 2.5-fold reduction in observed radioactivity, suggesting the formation of an electrophilic intermediate.

In an effort to confirm that the metabolic activation of **3** was unique to this compound and was not common among other members of the naphthamide family, compounds **20** and **22** were also profiled in rat and human microsomal incubations for bioactivation. As is illustrated in Table 7, compound **20** displayed a moderate potential for NADPH-dependent metabolic activation in both rat and human microsomes. In contrast,

Table 7. In Vitro Covalent Binding Measurements for ^{14}C-Labeled **3**, **20**, and **22**

	HLM[a] ((pmol/mg)/h)			RLM[a] ((pmol/mg)/h)		
compd	+NADPH	−NADPH	+NADPH + GSH	+NADPH	−NADPH	+NADPH + GSH
3	357	1.5	153	60	0.1	17
20	321	125	1.6	353	86	2.3
22	36	14	3.2	39	24	2.7

[a] 10 μM compound, 1 mg/mL protein, 1 h of incubation.

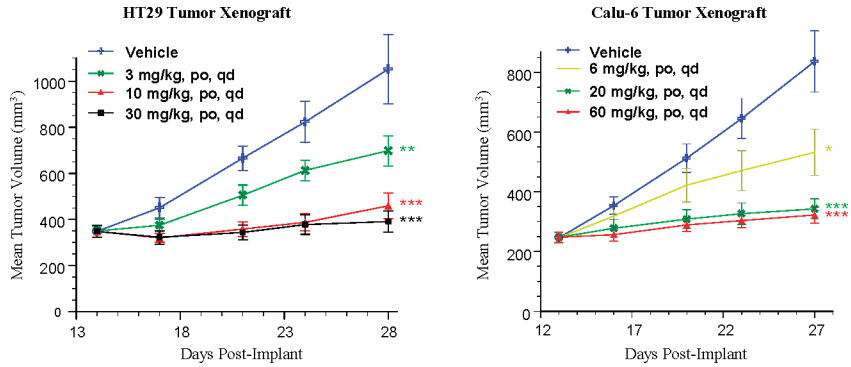

Figure 6. Antitumor activity upon treatment with **22** or vehicle in HT29 colon cancer xenograft and Calu-6 lung cancer xenograft in CD-1 nu/nu mice ($n = 10$ animals per group). Data represent the mean ± standard error: (∗) $P < 0.05$; (∗∗) $P < 0.01$; (∗∗∗) $P < 0.0001$.

Table 8. Plasma Protein Binding and Pharmacokinetic Parameters for **22** in Mouse, Dog, and Cyno

parameter	mouse	dog	cyno
plasma protein binding (%)	97.3	96.2	99.2
iv dose (mg/kg)	2[b]	0.5[d]	0.5[f]
po dose (mg/kg)	10[c]	0.5[e]	2
C_{max} (ng/mL), po	890	464	1049
T_{max} (h), po	0.25	0.75	0.83
AUC (ng·h/mL), po[a]	1498	3647	1358
$T_{1/2}$(h), po	5.6	16	13
MRT (h), iv	2.3	18	8.6
Cl ((mL/h)/kg), iv	2541	103	778
V_{ss} (mL/kg), iv	5739	1859	6823
F_{po} (%)	39	73	51

[a] $AUC_{(0-24\ h)}$. [b] Vehicle: Peg 400. [c] Vehicle: OraPlus. [d] Vehicle: DMSO. [e] Vehicle: 1% Tween-80, 2% HPMC, 97% water. [f] Vehicle: propylene glycol.

Table 9. In Vivo Antitumor Activity of **22** against Established Human HT29 Colon Cancer and Calu-6 Lung Cancer Xenografts Implanted Subcutaneously in CD-1 nu/nu Mice[a]

dose (mg/kg)[b]	TGI (%)[c]
HT29 Tumor Model	
3	51
10	85
30	94
Calu-6 Tumor Model	
6	52
20	85
60	88

[a] $n = 10$ animals per group. [b] Methanesulfonic acid (MSA) salt was dosed qd, po as a suspension in OraPlus. [c] Tumor growth inhibition.

compound **22** showed low levels of covalent binding in both rat and human microsomes, revealing a lower propensity to form reactive metabolites. The exact nature of the reactive intermediate generated from **20** is currently unclear.

The superior metabolic profile of **22** coupled with its promising in vivo efficacy led to an evaluation of its pharmacokinetic parameters in mouse, dog, and cynomolgous monkey (Table 8). Compound **22** demonstrated a moderate V_{ss} and low rate of clearance in dog, whereas in mouse and cynomolgous monkey, a somewhat elevated V_{ss} and higher rate of clearance relative to the hepatic blood flow for the respective species were observed. In each case, **22** was well absorbed following oral administration of drug from suspension formulations at the doses denoted in Table 8. The compound exhibited a moderate to slightly elongated half-life ($t_{1/2}$) of 5.6−16 h across the three species. Favorable mean residence times (MRT) were observed in mouse and cynomolgous monkey, with the values being slightly elevated in dog. The measured oral bioavailabilities were acceptable in all species and ranged from 39% to 73%.

In Vivo Tumor Xenograft Growth Inhibition. On the basis of its selectivity and promising pharmacokinetic profile across species, compound **22** was examined in the HT29 colon cancer and Calu-6 lung cancer xenograft models (Figure 6, Table 9). Cancer cells were implanted into the hind flank of female CD-1 nu/nu mice and allowed to establish for 12–14 days into sizable tumors, as determined by caliper measurements. In both xenograft models, once daily administration of **22** in OraPlus for 14 days led to antitumor efficacy in a dose-dependent fashion. In the HT29 xenograft model, 85% tumor growth inhibition was achieved at 10 mg/kg with an observed C_{max} of 1.3 μM and $AUC_{(0-24)}$ of 3.9 μM·h. A similar level of tumor growth inhibition was seen in the Calu-6 model at a dose of 20 mg/kg. No overt toxicity as measured by weight loss or morbidity was observed at any dose level throughout the dosing regimen.

Conclusion

N-Alkyl and *N*-unsubstituted naphthamides were prepared and identified as potent and selective inhibitors of KDR. Their enzyme inhibitory profiles translated well into endothelial cells, as exemplified by nanomolar inhibition of VEGF-driven HUVEC proliferation. Naphthamides **3**, **20**, and **22** exhibited good pharmacokinetics following oral dosing in rats and showed potent inhibition of VEGF-induced angiogenesis in the rat cornea. While compounds **3** and **20** suffered from metabolic activation and in turn led to moderate levels of covalent binding, **22** displayed a superior metabolic profile. Compound **22** showed a favorable PK profile in a range of species and once daily oral administration of **22** led to >85% inhibition of established HT29 colon cancer and Calu-6 lung cancer xenografts at doses of 10 and 20 mg/kg, respectively.

Experimental Section

Unless otherwise noted, all materials were obtained from commercial suppliers and used without further purification. Anhydrous solvents were purchased from Aldrich packaged under nitrogen in Sure/Seal bottles. Purity of final compounds was measured using Agilent 1100 series high-performance liquid chromatography (HPLC) systems with UV detection at 254 nm (system A consisting of Agilent Zorbax Eclipse XDB-C8 4.6 mm × 150 mm, 5 μm, 5–100% CH_3CN in H_2O with 0.1% TFA for 15 min at 1.5 mL/min; system B consisting of Waters Xterra 4.6 mm × 150 mm, 3.5 μm, 5–95% CH_3CN in H_2O with 0.1% TFA for 12 min at 1.0 mL/min). ^{1}H NMR spectra were recorded on a Bruker AV-4000 (400 MHz) spectrometer at ambient temperature. Chemical shifts are reported in ppm from the solvent resonance (DMSO-d_6 2.50 ppm). Data are reported as follows: chemical shift,

multiplicity (s = singlet, d = doublet, t = triplet, q = quartet, br = broad, m = multiplet), coupling constants, and number of protons. Low-resolution mass spectral (MS) data were determined on an Agilent 1100 series LCMS with UV detection at 254 nm and a low-resonance electrospray mode (ESI). High-resolution mass spectra were obtained on a high-resonance electrospray time-of-flight mass spectrometer. Combustion analysis was performed by Galbraith Laboratories, Inc., Knoxville, TN, and was within 0.4% of the calculated mass unless otherwise noted.

6,7-Dimethoxyquinolin-4-yloxy)-1-naphthoic Acid (5a). To a mixture of 6-hydroxy-1-napthoic acid (**4**) (14.34 g, 76.2 mmol) in 382 mL of dimethyl sulfoxide (DMSO) was added cesium carbonate (74.48 g, 228.6 mmol). After the mixture was stirred at room temperature for 15 min, 4-chloro-6,6-dimethoxyquinoline (20.46 g, 91.4 mmol) was added and the resulting mixture was heated at 140 °C for 3 h. The mixture was allowed to cool to room temperature and was poured into H_2O (200 mL). The pH was adjusted to 6.5 with 6 N HCl, and the resulting precipitate was filtered. The derived solid was washed sequentially with H_2O (2–250 mL), ether (2–250 mL), and CH_2Cl_2 (2–250 mL) to provide 6,7-dimethoxyquinolin-4-yloxy)-1-naphthoic acid (**5a**) (24.23 g, 85%) as a tan solid. ^{1}H NMR (400 MHz, DMSO-d_6) δ ppm 13.30 (brs, 1 H), 9.05 (d, J = 9.35 Hz, 1 H), 8.56 (d, J = 5.43 Hz, 1 H), 8.12–8.25 (m, 2 H), 7.95 (s, 1 H), 7.56–7.71 (m, 3 H), 7.48 (s, 1 H), 6.67 (d, J = 5.43 Hz, 1 H), 3.98 (s, 3 H), 3.96 (s, 3 H). HRMS $(C_{22}H_{18}NO_5)^+$: calcd, 376.117 95; found, 376.118 93.

6-(7-Methoxyquinolin-4-yloxy)-1-naphthoic Acid (5b). The title compound was prepared from 6-hydroxy-1-napthoic acid (**4**) using a method analogous to the preparation of compound **5a**. Yield: 807 mg, 82%. ^{1}H NMR (400 MHz, DMSO-d_6) δ ppm 13.28 (br s, 1 H), 9.04 (d, J = 9.35 Hz, 1 H), 8.65 (d, J = 5.18 Hz, 1 H), 8.25 (d, J = 9.22 Hz, 1 H), 8.18 (d, J = 7.71 Hz, 2 H), 7.91 (d, J = 2.65 Hz, 1 H), 7.59–7.68 (m, 2 H), 7.46 (d, J = 2.53 Hz, 1 H), 7.32 (dd, J = 9.16, 2.59 Hz, 1 H), 6.62 (d, J = 5.18 Hz, 1 H), 3.96 (s, 3 H). MS, m/z ($C_{21}H_{15}NO_4$): calcd, 345.1; found, 346.0 (MH).

6-(6-Carbamoyl-7-methoxyquinolin-4-yloxy)-1-naphthoic Acid (5c). A suspension of methyl 4-amino-2-methoxybenzoate (10.00 g, 55.19 mmol) in 200 mL of isopropanol was heated at 50 °C for 10 min at which point 5-(methoxymethylene)-2,2-dimethyl-1,3-dioxane-4,6-dione (9.64 g, 51.78 mmol) was added. The resulting suspension was heated at 80 °C for 1 h before being cooled to room temperature. The solid was filtered, washed well with ether, and dried in vacuo to provide methyl 4-((2,2-dimethyl-4,6-dioxo-1,3-dioxan-5-ylidene)methylamino)-2-methoxybenzoate (15.25 g, 82%) as a brown solid that was immediately processed. A suspension of the derived aniline (15.00 g, 53.96 mmol) in 135 mL of diphenyl ether was heated at 250 °C for 8 h. The mixture was cooled to room temperature and filtered. The resulting brown solid was washed with ether and dried in vacuo to provide methyl 7-methoxy-4-oxo-1,4-dihydroquinoline-6-carboxylate (9.60 g, 76%) as a brown solid that was used without further purification. The derived dihydroquinoline (5.00 g, 21.46 mmol) was added to 20 mL of thionyl chloride. Three drops of dimethylformamide (DMF) were added, and the mixture was heated at 125 °C for 3 h. The mixture was cooled to room temperature, and the solvent was removed in vacuo. The derived solid was taken up in CH_2Cl_2 (250 mL) and poured into saturated $NaHCO_3$ (500 mL). The layers were separated, and the aqueous layer was extracted with CH_2Cl_2 (250 mL). The combined organic layers were washed with brine, dried over sodium sulfate, filtered, and concentrated to provide a tan solid. Trituration of the solid with ether/hexanes provided methyl 4-chloro-7-methoxyquinoline-6-carboxylate (4.70 g, 87%) as a tan solid. The derived ester (1.00 g, 3.97 mmol) was added to ammonium hydroxide (20 mL), and the mixture was heated at 110 °C for 8 h before being cooled to room temperature. The mixture was filtered and the resulting solid was washed sequentially with water and ether to provide 4-chloro-7-methoxyquinoline-6-carboxamide (852 mg, 91%) as a tan solid. ^{1}H NMR (400 MHz, DMSO-d_6) δ ppm 8.82 (d, J = 4.80 Hz, 1 H), 8.49 (s, 1 H), 7.90 (br s, 1 H), 7.80 (br s, 1 H), 7.65 (d, J = 4.80 Hz, 1 H), 7.59 (s, 1 H), 4.03 (s, 3 H). The title compound was then prepared using a method analogous to the preparation of compound **5a**. Yield: 623 mg, 46%. ^{1}H NMR (400 MHz, DMSO-d_6) δ ppm 9.07 (d, J = 9.35 Hz, 1 H), 8.70–8.78 (m, 2 H), 8.20 (d, J = 7.58 Hz, 2 H), 7.99 (d, J = 2.40 Hz, 1 H), 7.93 (br s, 1 H), 7.80 (br s, 1 H), 7.63–7.71 (m, 2 H), 7.60 (s, 1 H), 6.71 (d, J = 5.43 Hz, 1 H), 4.07 (s, 3 H). MS, m/z ($C_{22}H_{16}N_2O_5$): calcd, 388.1; found, 389.1 (MH).

6-(6,7-Dimethoxyquinazolin-4-yloxy)-1-naphthoic Acid (8). The title compound was prepared from 6-hydroxy-1-napthoic acid (**4**) using a method analogous to the preparation of compound **5a**. Yield: 900 mg, 67%. ^{1}H NMR (400 MHz, DMSO-d_6) δ ppm 8.99 (d, J = 9.35 Hz, 1 H), 8.55 (s, 1 H), 8.16 (d, J = 7.45 Hz, 2 H), 7.98 (d, J = 2.40 Hz, 1 H), 7.55–7.69 (m, 3 H), 7.41 (s, 1 H), 4.01 (s, 3 H), 4.00 (s, 3 H). MS, m/z ($C_{21}H_{16}N_2O_5$): calcd, 376.1; found, 377.0 (MH).

***N*-Cyclopropyl-6-(6,7-dimethoxyquinolin-4-yloxy)-1-naphthamide (3).** To a solution of acid **5a** (2.50 g, 6.66 mmol) in 17 mL of DMF was added diisopropylethylamine (DIPEA) (4.64 mL, 26.6 mmol) followed by 2-(7-aza-1*H*-benzotriazole-1-yl)-1,1,3,3-tetramethyluronium hexafluorophosphate (HATU) (3.29 g, 8.66 mmol). After the mixture was stirred for 1 h, cyclopropylamine (923 μL, 13.3 mmol) was added and the mixture was maintained at room temperature for 8 h. The resulting mixture was filtered, and the resulting solid was washed sequentially with cold DMF and water. The solid was dried in vacuo to provide **3** (960 mg, 35%) as a white solid. The derived amine was taken up in ethanol and treated with 1 equiv of HCl (1 M in ether) to provide the hydrochloride salt as a white solid. HPLC purity: 98% (system A). ^{1}H NMR (400 MHz, DMSO-d_6) δ ppm 8.79 (d, J = 6.57 Hz, 1 H), 8.68 (d, J = 4.29 Hz, 1 H), 8.45 (d, J = 9.22 Hz, 1 H), 8.07 (d, 2 H), 7.82 (s, 1 H), 7.55–7.71 (m, 4 H), 6.90 (d, J = 6.44 Hz, 1 H), 4.06 (s, 6 H), 2.88–3.02 (m, 1 H), 0.69–0.81 (m, 2 H), 0.55–0.65 (m, 2 H). HRMS $(C_{25}H_{23}N_2O_4)^+$: calcd, 415.165 23; found, 415.164 66. Anal. ($C_{25}H_{22}N_2O_4 \cdot$HCl) C, H, N.

***N*-Cyclobutyl-6-(6,7-dimethoxyquinolin-4-yloxy)-1-naphthamide (10).** Thionyl chloride (10 mL) was added to acid **5a** (1.00 mg, 2.67 mmol), and the whole was heated at reflux for 1 h at which point the reaction was concentrated. The derived solid was azeotroped with benzene (20 mL) to provide the hydrochloride salt of the corresponding acid chloride (1.14 g, 100%) as a tan solid that was used without further purification. To a portion of the derived acid chloride (400 mg, 0.930 mmol) in 2.5 mL of CH_2Cl_2 were added DIPEA (810 μL, 4.65 mmol), cyclobutylamine (159 μL, 1.86 mmol), and a crystal of 4-dimethylaminopyridine (DMAP). Stirring was continued for 24 h at which point the mixture was diluted with 10 mL of dichloromethane and poured into 1 N NaOH. The layers were separated, and the organic layer was washed with brine, dried over sodium sulfate, filtered, and concentrated. Purification by silica gel chromatography (CH_3OH in CH_2Cl_2) or reverse-phase HPLC provided **10** (175 mg, 40%) as a white solid. HPLC purity: 99% (system A). ^{1}H NMR (400 MHz, DMSO-d_6) δ ppm 8.84 (d, J = 7.83 Hz, 1 H), 8.51 (d, J = 5.18 Hz, 1 H), 8.33 (d, J = 9.22 Hz, 1 H), 8.03 (dd, J = 6.76, 2.84 Hz, 1 H), 7.87 (d, J = 2.65 Hz, 1 H), 7.56–7.64 (m, 3 H), 7.54 (dd, J = 9.16, 2.46 Hz, 1 H), 7.44 (s, 1 H), 6.56 (d, J = 5.18 Hz, 1 H), 4.41–4.61 (m, 1 H), 3.97 (s, 3 H), 3.95 (s, 3 H), 2.22–2.36 (m, 2 H), 2.08 (t, J = 9.28 Hz, 2 H), 1.60–1.78 (m, 2 H). HRMS $(C_{26}H_{25}N_2O_4)^+$: calcd, 429.180 88; found, 429.180 33. Anal. ($C_{26}H_{24}N_2O_4 \cdot H_2O$) C, H, N.

***N*-Cyclopentyl-6-(6,7-dimethoxyquinolin-4-yloxy)-1-naphthamide (11).** The title compound was prepared from acid **5a** using a method analogous to the preparation of compound **10**. Yield: 113 mg, 24%. HPLC purity: 100% (system A); 99.1% (system B). ^{1}H NMR (400 MHz, DMSO-d_6) δ ppm 8.57 (d, J = 6.95 Hz, 1 H), 8.51 (d, J = 4.93 Hz, 1 H), 8.33 (d, J = 9.09 Hz, 1 H), 7.98–8.05 (m, 1 H), 7.86 (s, 1 H), 7.50–7.65 (m, 4 H), 7.44 (s, 1 H), 6.56 (d, J = 4.80 Hz, 1 H), 4.26–4.40 (m, 1 H), 3.97 (s, 3 H), 3.95 (s, 3 H), 1.90–2.03 (m, 2 H), 1.50–1.77 (m, 6 H). HRMS $(C_{27}H_{27}N_2O_4)^+$: calcd, 443.196 53; found, 443.196 10.

6-(6,7-Dimethoxyquinolin-4-yloxy)-*N*-(1-methylcyclopropyl)-1-naphthamide (12). The title compound was prepared from acid **5a** using a method analogous to the preparation of compound **10**. Yield: 70 mg, 16%. HPLC purity: 97% (system A); 97.8% (system

B). ^{1}H NMR (400 MHz, DMSO-d_6) δ ppm 8.79 (s, 1 H), 8.49 (d, 1 H), 8.31 (d, J = 9.35 Hz, 1 H), 8.00 (d, J = 8.08 Hz, 1 H), 7.85 (d, J = 2.27 Hz, 1 H), 7.48–7.61 (m, 4 H), 7.43 (s, 1 H), 6.54 (d, J = 5.31 Hz, 1 H), 3.96 (s, 3 H), 3.94 (s, 3 H), 1.47 (s, 3 H), 0.76–0.85 (m, 2 H), 0.58–0.70 (m, 2 H). HRMS $(C_{26}H_{25}N_2O_4)^+$: calcd, 429.180 88; found, 429.179 55.

***N*-(Cyclopropylmethyl)-6-(6,7-dimethoxyquinolin-4-yloxy)-1-naphthamide (13).** To a solution of the acid chloride derived from acid **5a** (120 mg, 0.305 mmol) and $NaHCO_3$ (76.8 mg, 0.914 mmol) in 5 mL of CH_2Cl_2 was added cyclopropylmethylamine (0.048 μL, 0.549 mmol). Upon complete consumption of starting material the reaction was quenched with saturated $NaHCO_3$ (25 mL). The layers were separated, and the aqueous layer was extracted with CH_2Cl_2 (2–10 mL). The combined organic layers were washed with brine, dried over sodium sulfate, and filtered. Concentration in vacuo and purification by silica gel chromatography (CH_3OH in CH_2Cl_2) provided **13** (66 mg, 51% yield) as an off-white solid. HPLC purity: 100% (system A). ^{1}H NMR (400 MHz, DMSO-d_6) δ ppm 8.63–8.75 (m, 1 H), 8.49 (d, J = 5.18 Hz, 1 H), 8.37 (d, J = 9.22 Hz, 1 H), 7.95–8.10 (m, 1 H), 7.86 (d, J = 2.40 Hz, 1 H), 7.49–7.65 (m, 4 H), 7.43 (s, 1 H), 6.55 (d, J = 5.18 Hz, 1 H), 3.96 (s, 3 H), 3.94 (s, 3 H), 3.24 (t, J = 6.19 Hz, 2 H), 1.03–1.17 (m, 1 H), 0.41–0.53 (m, 2 H), 0.23–0.35 (m, 2 H). HRMS $(C_{26}H_{25}N_2O_4)^+$: calcd, 429.180 88; found, 429.181 22. Anal. Calcd for $C_{26}H_{24}N_2O_4$: C, 72.88; H, 5.65; N, 6.54. Found: C, 73.37; H, 5.91; N, 6.40.

6-(6,7-Dimethoxyquinolin-4-yloxy)-*N*-methyl-1-naphthamide (14). The title compound was prepared from acid **5a** using a method analogous to the preparation of compound **10**. Yield: 129 mg, 33%. HPLC purity: 100% (system A). ^{1}H NMR (400 MHz, DMSO-d_6) δ ppm 8.53 (d, J = 4.67 Hz, 1 H), 8.50 (d, J = 5.18 Hz, 1 H), 8.38 (d, J = 9.22 Hz, 1 H), 8.03 (d, J = 7.71 Hz, 1 H), 7.86 (d, J = 2.53 Hz, 1 H), 7.55–7.64 (m, 3 H), 7.53 (dd, J = 9.28, 2.59 Hz, 1 H), 7.43 (s, 1 H), 6.56 (d, J = 5.18 Hz, 1 H), 3.97 (s, 3 H), 3.94 (s, 3 H), 2.87 (d, J = 4.67 Hz, 3 H). HRMS $(C_{23}H_{21}N_2O_4)^+$: calcd, 389.149 58; found, 389.147 39. Anal. ($C_{23}H_{20}N_2O_4$) C, H, N.

6-(6,7-Dimethoxyquinolin-4-yloxy)-*N*-ethyl-1-naphthamide (15). The title compound was prepared from acid **5a** using a method analogous to the preparation of compound **13**. Yield: 30 mg, 29%. HPLC purity: 100% (system A); 99.5% (system B). ^{1}H NMR (400 MHz, DMSO-d_6) δ ppm 8.54–8.64 (m, 1 H), 8.50 (d, J = 3.28 Hz, 1 H), 8.37 (d, J = 7.96 Hz, 1 H), 8.02 (d, J = 3.92 Hz, 1 H), 7.86 (s, 1 H), 7.49–7.64 (m, 4 H), 7.44 (s, 1 H), 6.56 (d, J = 3.41 Hz, 1 H), 3.97 (s, 3 H), 3.95 (s, 3 H), 3.30–3.43 (m, 2 H), 1.19 (t, J = 6.32 Hz, 3 H). HRMS $(C_{24}H_{23}N_2O_4)^+$: calcd, 403.165 23; found, 403.166 40.

6-(6,7-Dimethoxyquinolin-4-yloxy)-*N*-propyl-1-naphthamide (16). The title compound was prepared from acid **5a** using a method analogous to the preparation of compound **10**. Yield: 190 mg, 43%. HPLC purity: 98% (system A). ^{1}H NMR (400 MHz, DMSO-d_6) δ ppm 8.78 (d, J = 6.44 Hz, 1 H), 8.63 (t, J = 5.62 Hz, 1 H), 8.44 (d, J = 9.22 Hz, 1 H), 8.08 (d, J = 6.06 Hz, 1 H), 8.05 (d, J = 2.27 Hz, 1 H), 7.81 (s, 1 H), 7.59–7.71 (m, 4 H), 6.90 (d, J = 6.44 Hz, 1 H), 4.05 (s, 3 H), 4.05 (s, 3 H), 3.31 (q, J = 6.61 Hz, 2 H), 1.52–1.66 (m, 2 H), 0.96 (t, J = 7.39 Hz, 3 H). HRMS $(C_{25}H_{25}N_2O_4)^+$: calcd, 417.180 88; found, 417.181 36. Anal. ($C_{25}H_{24}N_2O_4 \cdot 3H_2O$) C, H, N.

6-(6,7-Dimethoxyquinolin-4-yloxy)-*N*-isopropyl-1-naphthamide (17). The title compound was prepared from acid **5a** using a method analogous to the preparation of compound **10**. Yield: 287 mg, 54%. HPLC purity: 99% (system A). ^{1}H NMR (400 MHz, DMSO-d_6) δ ppm 8.49 (d, J = 5.18 Hz, 1 H), 8.46 (d, J = 7.58 Hz, 1 H), 8.33 (d, J = 9.22 Hz, 1 H), 8.01 (dd, J = 6.44, 3.16 Hz, 1 H), 7.86 (d, J = 2.53 Hz, 1 H), 7.55–7.62 (m, 3 H), 7.53 (dd, J = 9.28, 2.59 Hz, 1 H), 7.43 (s, 1 H), 6.54 (d, J = 5.31 Hz, 1 H), 4.10–4.24 (m, 1 H), 3.96 (s, 3 H), 3.94 (s, 3 H), 1.23 (s, 3 H), 1.21 (s, 3 H). HRMS $(C_{25}H_{25}N_2O_4)^+$: calcd, 417.180 88; found, 417.181 32. Anal. ($C_{25}H_{24}N_2O_4$) C, H, N.

***N*-*tert*-Butyl-6-(6,7-dimethoxyquinolin-4-yloxy)-1-naphthamide (18).** To a solution of 6-hydroxynapthoic acid (1.00 g, 5.32 mmol) in 10 mL of CH_2Cl_2 was added 1-ethyl-3-(3-dimethylaminopropyl)carbodiimide hydrochloride (EDC) (1.20 g, 6.38 mmol), 1-hydroxy-7-azabenzotriazole (HOAt) (10.6 mL, 0.6 M in DMF), *tert*-butylamine (388 mg, 5.32 mmol), and DIPEA (1.40 mL, 7.98 mmol). The mixture was maintained at room temperature for 8 h at which point the mixture was concentrated in vacuo and purified by silica gel chromatography (CH_3OH in CH_2Cl_2) to provide *N*-*tert*-butyl-6-hydroxynaphthamide (550 mg, 46%) as a light-pink solid. The derived amide (200 mg, 0.82 mmol) was dissolved in 1 mL of pyridine and 1.5 mL of DMF, and Cu (8.0 mg, 0.04 mmol) and potassium hydroxide 94 mg, 2.6 mmol) were added. The mixture was heated to 120 °C in a microwave for 20 min before being diluted with 10 mL of $CHCl_3$ and poured into 1 N NaOH (10 mL). The aqueous layer was extracted with $CHCl_3$ (3 × 10 mL). The combined aqueous layers were washed with water and brine and dried over sodium sulfate. Filtration and concentration provided a residue that was purified by silica gel chromatography CH_3OH in CH_2Cl_2) to provide *N*-*tert*-butyl-6-(6,7-dimethoxyquinolin-4-yloxy)-1-naphthamide (**18**, 115 mg, 32%) as an off-white solid. HPLC purity: 97% (system A). ^{1}H NMR (400 MHz, DMSO-d_6) δ ppm 8.49 (d, J = 5.31 Hz, 1 H), 8.26 (d, J = 9.22 Hz, 1 H), 8.17 (s, 1 H), 7.98 (d, J = 7.96 Hz, 1 H), 7.84 (d, J = 2.53 Hz, 1 H), 7.49–7.62 (m, 4 H), 7.43 (s, 1 H), 6.53 (d, J = 5.18 Hz, 1 H), 3.96 (s, 3 H), 3.94 (s, 3 H), 1.45 (s, 9 H). HRMS $(C_{26}H_{27}N_2O_4)^+$: calcd, 431.196 53; found, 431.196 04. Anal. ($C_{26}H_{26}N_2O_4 \cdot CH_2Cl_2$) C, H, N.

6-(6,7-Dimethoxyquinolin-4-yloxy)-*N*-(2,2,2-trifluoroethyl)-1-naphthamide (19). The title compound was prepared from acid **5a** using a method analogous to the preparation of compound **13**. Yield: 65 mg, 47%. HPLC purity: 100% (system A). ^{1}H NMR (400 MHz, DMSO-d_6) δ ppm 9.30 (t, J = 6.32 Hz, 1 H), 8.50 (d, J = 5.18 Hz, 1 H), 8.30 (d, J = 9.22 Hz, 1 H), 8.08 (d, J = 6.69 Hz, 1 H), 7.89 (d, J = 2.53 Hz, 1 H), 7.51–7.70 (m, 4 H), 7.43 (s, 1 H), 6.57 (d, J = 5.18 Hz, 1 H), 4.10–4.28 (m, 2 H), 3.96 (s, 3 H), 3.94 (s, 3 H). HRMS $(C_{24}H_{20}F_3N_2O_4)^+$: calcd, 457.137 52; found, 457.137 69. Anal. ($C_{24}H_{19}F_3N_2O_4 \cdot CH_3OH$) C, H, N.

6-(6,7-Dimethoxyquinolin-4-yloxy)-*N*-(2-methoxyethyl)-1-naphthamide (20). The title compound was prepared from acid **5a** using a method analogous to the preparation of compound **10**. Yield: 190 mg, 21%. HPLC purity: 100% (system A). ^{1}H NMR (400 MHz, DMSO-d_6) δ ppm 8.63 (t, J = 4.80 Hz, 1 H), 8.49 (d, J = 5.18 Hz, 1 H), 8.36 (d, J = 9.35 Hz, 1 H), 8.02 (dd, J = 5.94, 3.41 Hz, 1 H), 7.86 (d, J = 2.53 Hz, 1 H), 7.55–7.62 (m, 3 H), 7.53 (dd, J = 9.22, 2.53 Hz, 1 H), 7.43 (s, 1 H), 6.55 (d, J = 5.18 Hz, 1 H), 3.96 (s, 3 H), 3.94 (s, 3 H), 3.47–3.55 (m, 4 H), 3.32 (s, 3 H). HRMS $(C_{25}H_{25}N_2O_5)^+$: calcd, 433.175 80; found, 433.175 81. Anal. ($C_{25}H_{24}N_2O_4 \cdot 0.33CH_3OH$) C, H, N.

6-(6,7-Dimethoxyquinolin-4-yloxy)-*N*-(3-methoxypropyl)-1-naphthamide (21). The title compound was prepared from acid **5a** using a method analogous to the preparation of compound **10**. Yield: 246 mg, 52%. HPLC purity: 100% (system A). ^{1}H NMR (400 MHz, DMSO-d_6) δ ppm 8.59 (t, J = 5.24 Hz, 1 H), 8.49 (d, J = 5.18 Hz, 1 H), 8.35 (d, J = 9.22 Hz, 1 H), 8.02 (dd, J = 6.88, 2.59 Hz, 1 H), 7.86 (d, J = 2.40 Hz, 1 H), 7.55–7.64 (m, 3 H), 7.53 (dd, J = 9.28, 2.46 Hz, 1 H), 7.43 (s, 1 H), 6.56 (d, J = 5.18 Hz, 1 H), 3.96 (s, 3 H), 3.94 (s, 3 H), 3.44 (t, J = 6.32 Hz, 2 H), 3.38 (q, J = 6.65 Hz, 2 H), 3.30 (s, 2 H), 3.27 (s, 3 H), 1.73–1.88 (m, 2 H). HRMS $(C_{26}H_{27}N_2O_5)^+$: calcd, 447.191 45; found, 447.190 68. Anal. ($C_{26}H_{26}N_2O_5 \cdot 0.33CH_3OH$) C, H, N.

6-(6,7-Dimethoxyquinolin-4-yloxy)-1-naphthamide methanesulfonate (22). The title compound was prepared from acid **5a** using a method analogous to the preparation of compound **10**. The derived amine was taken up in ethanol, treated with 1 equiv of methanesulfonic acid (MSA), and concentrated to provide the methanesulfonate salt of the derived amine. Yield: 180 mg, 46%. HPLC purity: 99% (system A). ^{1}H NMR (400 MHz, DMSO-d_6) δ ppm 8.80 (d, J = 6.57 Hz, 1 H), 8.59 (d, J = 9.35 Hz, 1 H), 8.01–8.13 (m, 2 H), 7.83 (s, 1 H), 7.76 (d, J = 7.07 Hz, 1 H), 7.60–7.72 (m, 2 H), 7.57 (s, 1 H), 6.93 (d, J = 6.57 Hz, 1 H), 4.06 (s, 3 H), 4.05 (s, 3 H), 3.34–3.65 (br s, 2 H), 2.31 (s, 3 H). HRMS $(C_{22}H_{19}N_2O_4)^+$:

calcd, 375.133 93; found, 375.134 29. Anal. ($C_{22}H_{18}N_2O_4 \cdot CH_3SO_3H$) C, H, N.

***N*-Cyclopropyl-6-(6,7-dimethoxyquinazolin-4-yloxy)-1-naphthamide (23).** The title compound was prepared from 6-(6,7-dimethoxyquinazolin-4-yloxy)-1-naphthoic acid using a method analogous to the preparation of compound **13**. Yield: 16 mg, 24%. HPLC purity: 99% (system A). ^{1}H NMR (400 MHz, DMSO-d_6) δ ppm 8.64 (d, J = 4.55 Hz, 1 H), 8.54 (s, 1 H), 8.28 (d, J = 9.09 Hz, 1 H), 8.02 (t, J = 4.86 Hz, 1 H), 7.93 (d, J = 2.40 Hz, 1 H), 7.64 (s, 1 H), 7.53–7.60 (m, 2 H), 7.42 (s, 1 H), 4.01 (s, 3 H), 4.00 (s, 3 H), 2.92–2.99 (m, 1 H), 0.71–0.78 (m, 2 H), 0.60–0.64 (m, 2 H). HRMS $(C_{24}H_{22}N_3O_4)^+$: calcd, 416.161 03; found, 416.161 13. Anal. ($C_{24}H_{21}N_3O_4$) C, H, N.

6-(6,7-Dimethoxyquinazolin-4-yloxy)-*N*-(2-methoxyethyl)-1-naphthamide (24). The title compound was prepared from (6,7-dimethoxyquinazolin-4-yloxy)-1-naphthoic acid using a method analogous to the preparation of compound **13**. Yield: 45 mg, 68%. HPLC purity: 100% (system A). ^{1}H NMR (400 MHz, DMSO-d_6) δ ppm 8.65 (t, J = 4.67 Hz, 1 H), 8.54 (s, 1 H), 8.31 (d, J = 9.22 Hz, 1 H), 8.03 (dd, J = 5.75, 3.73 Hz, 1 H), 7.93 (d, J = 2.27 Hz, 1 H), 7.58–7.66 (m, 3 H), 7.56 (dd, J = 9.22, 2.40 Hz, 1 H), 7.42 (s, 1 H), 4.00 (d, J = 1.01 Hz, 6 H), 3.46–3.58 (m, 4 H), 3.32 (s, 3 H). HRMS $(C_{24}H_{24}N_3O_5)^+$: calcd, 434.171 05; found, 434.171 31. Anal. ($C_{24}H_{23}N_3O_5$) C, H, N.

6-(6,7-Dimethoxyquinazolin-4-yloxy)-1-naphthamide (25). The title compound was prepared from (6,7-dimethoxyquinazolin-4-yloxy)-1-naphthoic acid using a method analogous to the preparation of compound **13**. The crude derived solid was rinsed well with water and methanol to provide **25** (17 mg, 53%) as a white solid. HPLC purity: 96% (system A). ^{1}H NMR (400 MHz, DMSO-d_6) δ ppm 8.54 (s, 1 H), 8.42 (br s, 1 H), 7.98–8.13 (m, 2 H), 7.93 (s, 1 H), 7.49–7.73 (m, 3 H), 7.42 (s, 1 H), 4.00 (s, 6 H), 3.21–3.39 (br s, 2 H). HRMS $(C_{21}H_{18}N_3O_4)^+$: calcd, 376.129 18; found, 376.127 95. Anal. Calcd for $C_{21}H_{17}N_3O_4$: N, 67.19; H, 4.56; N, 11.19. Found: C, 66.04; H, 4.51; N, 9.67.

***N*-Cyclopropyl-6-(7-methoxyquinolin-4-yloxy)-1-naphthamide (26).** The title compound was prepared from 6-(7-methoxyquinolin-4-yloxy)-1-naphthoic acid (**5b**) using a method analogous to the preparation of compound **13**. Yield: 73 mg, 69%. HPLC purity: 100% (system A). ^{1}H NMR (400 MHz, DMSO-d_6) δ ppm 8.59–8.67 (m, 2 H), 8.34 (d, J = 9.22 Hz, 1 H), 8.24 (d, J = 9.22 Hz, 1 H), 8.01 (t, J = 4.80 Hz, 1 H), 7.85 (d, J = 2.40 Hz, 1 H), 7.58 (d, J = 4.93 Hz, 2 H), 7.53 (dd, J = 9.16, 2.46 Hz, 1 H), 7.44 (d, J = 2.53 Hz, 1 H), 7.31 (dd, J = 9.03, 2.46 Hz, 1 H), 6.57 (d, J = 5.18 Hz, 1 H), 3.95 (s, 3 H), 3.32 (s, 1 H), 0.69–0.78 (m, 2 H), 0.56–0.64 (m, 2 H). HRMS $(C_{24}H_{21}N_2O_3)^+$: calcd, 385.154 67; found, 385.155 13. Anal. Calcd for $C_{24}H_{20}N_2O_3$: C, 74.98; H, 5.24; N, 7.29. Found: C, 74.97; H, 5.74; N, 7.27.

***N*-(2-Methoxyethyl)-6-(7-methoxyquinolin-4-yloxy)-1-naphthamide (27).** The title compound was prepared from 6-(7-methoxyquinolin-4-yloxy)-1-naphthoic acid (**5b**) using a method analogous to the preparation of compound **13**. Yield: 68 mg, 62%. HPLC purity: 99% (system A). ^{1}H NMR (400 MHz, DMSO-d_6) δ ppm 8.60–8.67 (m, 2 H), 8.36 (d, J = 9.22 Hz, 1 H), 8.24 (d, J = 9.22 Hz, 1 H), 8.02 (dd, J = 6.00, 3.35 Hz, 1 H), 7.86 (d, J = 2.53 Hz, 1 H), 7.57–7.62 (m, 2 H), 7.53 (dd, J = 9.22, 2.40 Hz, 1 H), 7.44 (d, J = 2.53 Hz, 1 H), 7.31 (dd, J = 9.22, 2.53 Hz, 1 H), 6.57 (d, J = 5.18 Hz, 1 H), 3.95 (s, 3 H), 3.46–3.57 (m, 4 H), 3.32 (s, 3 H). HRMS $(C_{24}H_{23}N_2O_4)^+$: calcd, 403.165 23; found, 403.166 40. Anal. ($C_{24}H_{22}N_2O_4 \cdot 0.5CH_3OH$) C, H, N.

6-(7-Methoxyquinolin-4-yloxy)-1-naphthamide (28). The title compound was prepared from 6-(7-methoxyquinolin-4-yloxy)-1-naphthoic acid (**5b**) using a method analogous to the preparation of compound **13**. Yield: 31 mg, 56%. HPLC purity: 99% (system A). ^{1}H NMR (400 MHz, DMSO-d_6) δ ppm 8.63 (d, J = 5.18 Hz, 1 H), 8.47 (d, J = 9.22 Hz, 1 H), 8.24 (d, J = 9.09 Hz, 1 H), 8.06 (br s, 1 H), 8.01 (d, J = 8.21 Hz, 1 H), 7.85 (d, J = 2.53 Hz, 1 H), 7.62–7.70 (m, 2 H), 7.59 (d, J = 7.71 Hz, 1 H), 7.54 (dd, J = 9.22, 2.40 Hz, 1 H), 7.44 (d, J = 2.40 Hz, 1 H), 7.31 (dd, J = 9.16, 2.46 Hz, 1 H), 6.58 (d, J = 5.18 Hz, 1 H), 3.95 (s, 3 H). HRMS $(C_{21}H_{17}N_2O_3)^+$: calcd, 345.123 37; found, 345.122 81. Anal. ($C_{21}H_{16}N_2O_3 \cdot 0.5CH_3OH$) C, H, N.

4-(5-(Cyclopropylcarbamoyl)naphthalen-2-yloxy)-7-methoxyquinoline-6-carboxamide (29). The title compound was prepared from 6-(6-carbamoyl-7-methoxyquinolin-4-yloxy)-1-naphthoic acid (**5c**) using a method analogous to the preparation of compound **10**. Yield: 189 mg, 55%. HPLC purity: 99% (system A). ^{1}H NMR (400 MHz, DMSO-d_6) δ ppm 8.72 (s, 1 H), 8.68 (d, J = 5.18 Hz, 1 H), 8.64 (d, J = 4.42 Hz, 1 H), 8.35 (d, J = 9.09 Hz, 1 H), 7.97–8.05 (m, 1 H), 7.89 (d, J = 2.40 Hz, 1 H), 7.88 (br s, 1 H), 7.75 (br s, 1 H), 7.51–7.61 (m, 4 H), 6.59 (d, J = 5.18 Hz, 1 H), 4.04 (s, 3 H), 2.89–3.01 (m, 1 H), 0.74 (dd, J = 7.07, 2.27 Hz, 2 H), 0.55–0.64 (m, 2 H). HRMS $(C_{25}H_{22}NaN_3O_4)^+$: calcd, 450.142 43; found, 450.142 75. Anal. ($C_{25}H_{21}N_3O_4 \cdot CH_3OH$) C, H, N.

4-(5-((2-Methoxyethyl)carbamoyl)naphthalen-2-yloxy)-7-methoxyquinoline-6-carboxamide (30). The title compound was prepared from 6-(6-carbamoyl-7-methoxyquinolin-4-yloxy)-1-naphthoic acid (**5c**) using a method analogous to the preparation of compound **10**. Yield:153 mg, 70%. HPLC purity: 100% (system A). ^{1}H NMR (400 MHz, DMSO-d_6) δ ppm 8.73 (s, 1 H), 8.69 (d, J = 5.18 Hz, 1 H), 8.65 (t, J = 5.18 Hz, 1 H), 8.38 (d, J = 9.35 Hz, 1 H), 8.03 (dd, J = 5.75, 3.85 Hz, 1 H), 7.91 (d, J = 2.53 Hz, 1 H), 7.88 (br s, 1 H), 7.76 (br s, 1 H), 7.53–7.64 (m, 4 H), 6.60 (d, J = 5.18 Hz, 1 H), 4.05 (s, 3 H), 3.46–3.56 (m, 4 H), 3.32 (s, 3 H). HRMS $(C_{25}H_{24}N_3O_5)^+$: calcd, 446.171 05; found, 446.171 16. Anal. ($C_{25}H_{23}N_3O_5 \cdot 0.5CH_3OH$) C, H, N.

4-(5-Carbamoylnaphthalen-2-yloxy)-7-methoxyquinoline-6-carboxamide (31). The title compound was prepared from 6-(6-carbamoyl-7-methoxyquinolin-4-yloxy)-1-naphthoic acid (**5c**) using a method analogous to the preparation of compound **10**. Yield: 75 mg, 76%. HPLC purity: 100% (system A). ^{1}H NMR (400 MHz, DMSO-d_6) δ ppm 8.72 (s, 1 H), 8.68 (d, J = 5.18 Hz, 1 H), 8.48 (d, J = 9.35 Hz, 1 H), 8.07 (s, 1 H), 8.02 (d, J = 8.21 Hz, 1 H), 7.89 (d, J = 2.53 Hz, 1 H), 7.87 (s, 1 H), 7.75 (s, 1 H), 7.64–7.70 (m, 2 H), 7.60 (d, J = 7.83 Hz, 1 H), 7.52–7.58 (m, 2 H), 6.60 (d, J = 5.18 Hz, 1 H), 4.05 (s, 3 H). HRMS $(C_{22}H_{18}N_3O_4)^+$: calcd, 388.129 18; found, 388.128 90. Anal. ($C_{22}H_{17}N_3O_4 \cdot 0.5CH_3OH$) C, H, N.

VEGFR-2 Kinase Assay.[16] In a 96-well plate, 5 nM/L of either the phosphorylated or nonphosphorylated form of the VEGFR-2 kinase domain was incubated with compound (10-point titration ranging from 3 μM to 0.15 nM), 1 μM/L gastrin substrate, 20 mM/L Tris-HCl, pH 7.5, 10 mM/L $MgCl_2$, 100 mM/L NaCl, 1.5 mM/L EGTA, 1 mM/L DTT, 0.2 mM/L sodium orthovanadate, and 20 μg/mL BSA for 30 min at 25 °C. ATP was added at a final concentration of 11.8 μM and incubated for 60 min at room temperature. Eu-labeled antiphosphotyrosine pT66 antibody (Perkin-Elmer) was then used for detection.

HUVEC Proliferation Assay.[16] Cells were cultured in endothelial growth medium-2 (Cambrex). HUVECs were seeded into flat-bottom, 96-well plates (BD Falcon) at 3000 cells per well in Dulbecco's modified Eagle's medium (DMEM) with 10% fetal bovine serum (FBS), penicillin, and streptomycin. After culture for 22 h, media were removed and cells were preincubated for 2 h with serial dilutions of compound diluted 1:400 in DMEM with 10% FBS plus penicillin/streptomycin. HUVECs were then challenged with 50 ng/mL VEGF or 20 ng/mL bFGF and incubated for 72 h at 37 °C, 5% CO_2. Cells were washed twice with DPBS, and plates were frozen at −70 °C for 24 h. Plates were thawed, incubated with CyQuant dye (Molecular Probes), and read on a Victor 1420 workstation (Perkin-Elmer Corporation). IC_{50} data were calculated using the Levenburg−Marquardt algorithm in a four-parameter logistic equation (ID Business Solutions Ltd., Alameda, CA).

In Vitro Metabolism and CL_{int} Calculations. The in vitro intrinsic clearances, CL_{int}, of the test compounds were determined by incubations with human and rat liver microsomes purchased from BD Biosciences (San Jose, CA). The 400 μL incubations contained 0.25 mg of microsomal protein/mL, 1 mM NADPH, 2 mM $MgCl_2$ in 50 mM potassium phosphate buffer, pH 7.4. Test compounds were added to the prewarmed (37 °C) incubation mixtures at the

final concentration of 1 μM. At 0, 10, 20, 30, and 40 min following addition of test compound, aliquots of the incubation mixture (35 μL) were collected into an equal volume of acetonitrile plus internal standard (1 μM tolbutamide). The samples were centrifuged at 3500*g* for 15 min and analyzed on a liquid chromatography tandem mass spectrometry system consisting of two Shimadzu LC-10AD HPLC pumps and a DGU-14A degasser (Shimadzu, Columbia, MD), CTC PAL autoinjector (Leap Technologies, Carrboro, NC), and an API3000 LC−MSMS system. Chromatography was conducted on a Sprite Armor C18 (20 mm × 2.1 mm, 10 μm) analytical column (Analytical Sales and Products, Pompton Plains, NJ) with a 0.5 μm PEEK guard filter, using the following mobile phase gradient program: MPA = H_20 with 0.1% formic acid; MPB = acetonitrile with 0.1% formic acid; 0 min = 98% MPA, 2% MPB; 0.3 min = 98% MPA, 2% MPB; 0.7 min = 5% MPA, 95% MPB; 1.3 min = 5% MPA, 95% MPB; 1.4 min = 98% MPA, 2% MPB; 1.7 min = end of run; approximately 2 min between sample injections. For each compound, peak areas at each time point were converted to the natural log of the percentage remaining relative to the 0 min samples.[29] The resulting slope of these values relative to time (k) was converted to in vitro $T_{1/2}$ where $T_{1/2} = -0.693/k$. CL_{int} was calculated using the following relationship: $CL_{int} = (0.693/T_{1/2})(1/0.25 \text{ mg/mL})$.

In Vivo Vascular Permeability Assay. Vascular permeability was induced using a modified Miles assay[30] and was conducted as previously described.[16]

Rat Corneal Angiogenesis Model. Corneal angiogenesis was evaluated in adult female Sprague–Dawley rats as previously described.[31]

Pharmacokinetic Studies. Male Sprague–Dawley rats were dosed via femoral vein (intravenous, DMSO solution, dose 1 mg/kg) or via oral gavage (suspensions in OraPlus, pH adjusted to a range of 2.0–2.2 using methanesulfonic acid, dose 10 mg/kg). Concentrations of all formulations were selected to allow for dose volumes in accordance with the highest scientific, humane, and ethical principals as defined by IACUC (Institutional Animal Care and Use Committees). Serial blood samples were collected from jugular vein into heparized tubes over a 12–24 h period. Plasma was separated by centrifugation, and the sample was prepared for analysis by protein precipitation with acetonitrile. Quantitation of the test compounds was accomplished by reverse-phase liquid chromatography with mass spectral detection in multiple reaction monitoring mode, with an appropriate internal standard. Pharmacokinetic parameters such as clearance, volume of distribution, and terminal half-life were calculated by a noncompartmental method.

Tumor Xenograft Models. Both the Calu-6 and HT29 cell lines were originally obtained from ATCC. HT29 cells were maintained at 37 °C in DMEM high glucose, 5% FBS, 1× NEAA, 2 mM L-glutamine (Gibco/BRL, Grand Island, NY) under standard tissue culture conditions. In like manner, Calu-6 cells were maintained in RPMI 1640 10% FBS, 1× NEAA, 2 mM L-glutamine (Gibco/BRL, Grand Island, NY). CD1 nu/nu mice within approximately 4–8 weeks of age were challenged with subcutaneous implants of cultured HT29 (human colon carcinoma) or Calu-6 (human NSCLC) cells (1×10^7 cells per mouse). After 13−14 days, when tumors had reached approximately 300 mm^3, animals began continuous daily treatment with compound **22** administered po, qd at the indicated dose levels. Tumor volumes as established by caliper measurements were recorded twice per week, along with body weights as an index of toxicity. Data are expressed as mean values plus or minus standard errors as a function of time. Statistical significance of observed differences was evaluated by repeated measures analysis of variance (RMANOVA) followed by Scheffé post hoc testing for multiple comparisons.

Covalent Binding Studies. Human and rat liver microsomes (20 mg/mL) were purchased from Xenotech, LLC (Lenexa, KS). NADPH and glutathione were purchased from Sigma-Aldrich Chemical Co. (St. Louis, MO). $H_2{}^{18}O$ was ordered from Cambridge Isotope Laboratories Inc. (Andover, MA), and SOLVABLE was purchased from Perkin-Elmer Life Sciences (Boston, MA).

Microsomal Incubations. ^{14}C compound (10 μM) and liver microsomes (1 mg/mL) were mixed with 0.1 M potassium phosphate buffer (pH 7.4) for a final volume of 0.5 mL. The samples were preincubated at 37 °C for 3 min, and then 1 mM NADPH was added. The incubations were quenched with 1.0 mL of ice-cold acetonitrile after 60 min followed by vortex mixing and centrifugation. The supernatant was dried under a steady stream of N_2 and reconstituted in the initial mobile phase described below. A 50 μL injection was made using the LCMS method described below.

In Vitro Covalent Binding Assay. ^{14}C compound (10 μM) was again incubated with liver microsomes (1 mg/mL), (±)-glutathione (1 mM), 0.1 M potassium phosphate buffer (pH 7.4), and NADPH (1 mM) in a final volume of 0.2 mL The incubations were quenched with 0.4 mL of ice-cold acetonitrile after 60 min followed by vortex mixing, centrifugation, and removal of the supernatant. The pellet was washed three times with 80% methanol, twice with 3:1 ethanol/ether, and twice with 80% methanol. The total radioactivity in the final supernatant was determined by liquid scintillation counting and was not more than background. The pellet was dried overnight and then solubilized in 0.5 mL of 60% SOLVABLE. The protein concentration was determined using a standard BCA protein assay, and 0.375 mL of the solubilized protein was used for liquid scintillation counting

LCMS Assay. HPLC analyses were carried out on an Agilent 1100 gradient system (Palo Alto, CA). Separation was achieved on a Waters YMC ODS-AQ 4.6 mm × 150 mm column with a flow rate of 1 mL/min. The mobile phase consisted of 0.1% formic acid in water (A) and 0.1% formic acid in acetonitrile (B). The gradient started at 95% A and linearly ramped to 50% A over 30 min. The flow was split so that 0.8 mL/min flowed through an INUS β-RAM (Rivera Beach, FL; scintillation cocktail flow rate of 2.4 mL/min) and 0.2 mL/min flowed into a Thermo Electron ion trap mass spectrometer (LCQ-Deca XP plus or LTQ; San Jose, CA).

Protein Binding Assay. Plasma filtrate was used for the calibration curve and QC samples. To generate plasma filtrate, an aliquot of plasma was filtered through Millipore Centriplus (a filter) by spinning at 3000*g* (4980 rpm) at 4 °C for 24 h with a Beckman Avanti J-251 ultracentrifuge. An aliquot of 10 μL of test compound (1 mg/mL in DMSO) was added to 1990 μL of human, rat, dog, and mouse plasma to give a final concentration of 5 mg/mL (12.9 μM). Separate QC samples were prepared by adding 10 μL of the test compound spiked plasma sample (5 μg/mL) to 490 μL of plasma filtrate, in duplicate. The plasma samples including the QC samples were then incubated at 37 °C for 15 min. Following incubation, 800 μL was transferred to the centrifuge tube (in duplicate) and spun at 120 000 rpm for 3 h at 37 °C with a TLA-120.2 rotor (Optima TLX ultracentrifuge, Beckman Coulter). The top portion below the lipid layer of the centrifuged plasma sample was aspirated (100 μL in triplicate) for LCMS analysis. The QC samples (100 μL in duplicate) were also aspirated for LCMS analysis. The concentrations of the samples ($n = 6$) and QCs ($n = 2$) were determined from a linear regression of peak area ratios (analyte peak area/IS peak area) versus the theoretical concentrations of the calibration standards. The percent of binding was calculated as

$$\% \text{ protein binding} = 1 - (\text{concentration of the centrifuged plasma sample})/(\text{mean concentration of the QC}) \times 100$$

Acknowledgment. We thank our colleagues Angela Bretz and Victor Chi in PKDM, and Ingrid Fellows for the preparation of compound **18**.

Supporting Information Available: Tables of elemental analysis, HPLC anlysis, and X-ray data. This material is available free of charge via the Internet at http://pubs.acs.org.

References

(1) (a) Folkman, J. Anti-angiogenesis: new concept for therapy of solid tumors. *Ann. Surg.* **1972**, *175*, 409–416. (b) Ferrara, N. VEGF and

the quest for tumour angiogenesis factors. *Nat. Rev. Cancer* **2002**, *2*, 795–803.

(2) (a) Cherrington, J. M.; Strawn, L. M.; Shawver, L. K. New paradigms for the treatment of cancer: the role of anti-angiogenesis agents. *Adv. Cancer Res.* **2000**, *79*, 1–38. (b) Siemann, D. W.; Chaplin, D. J.; Horsman, M. R. Vascular-targeting therapies for treatment of malignant disease. *Cancer* **2004**, *100*, 2491–2499.

(3) Carmeliet, P. Mechanisms of angiogenesis and arteriogenesis. *Nat. Med.* **2000**, *6*, 389–395.

(4) Rak, J.; Mitsuhashi, Y.; Bayko, L.; Filmus, J.; Shirasawa, S.; Sasazuki, T.; Kerbel, R. S. Mutant ras oncogenes upregulate VEGF/VPF expression: implications for induction and inhibition of tumor angiogenesis. *Cancer Res.* **1995**, *55*, 4575–4580.

(5) Mukhopadhyay, D.; Knebelmann, B.; Cohen, H. T.; Ananth, S.; Sukhatme, V. P. The von Hippel−Lindau tumor suppressor gene product interacts with Sp1 to repress vascular endothelial growth factor promoter activity. *Mol. Cell. Biol.* **1997**, *17*, 5629–5639.

(6) Shweiki, D.; Neeman, M.; Itin, A.; Keshet, E. Induction of vascular endothelial growth factor expression by hypoxia and by glucose deficiency in multicell spheroids: implications for tumor angiogenesis. *Proc. Natl. Acad. Sci. U.S.A.* **1995**, *92*, 768–772.

(7) Wiesmann, C.; Fuh, G.; Christinger, H. W.; Eigenbrot, C.; Wells, J. A.; de Vos, A. M. Crystal structure at 1.7 Å resolution of VEGF in complex with domain 2 of the Flt-1 receptor. *Cell* **1997**, *91*, 695–704.

(8) Terman, B. I.; Dougher-Vermazen, M.; Carrion, M. E.; Dimitrov, D.; Armellino, D. C.; Gospodarowicz, D.; Bohlen, P. Identification of the KDR tyrosine kinase as a receptor for vascular endothelial cell growth factor. *Biochem. Biophys. Res. Commun.* **1992**, *187*, 1579–1586.

(9) Kim, K. J.; Li, B.; Winer, J.; Armanini, M.; Gillett, N.; Phillips, H. S.; Ferrara, N. Inhibition of vascular endothelial growth factor-induced angiogenesis suppresses tumour growth in vivo. *Nature* **1993**, *362*, 841–844.

(10) (a) Hurwitz, H.; Fehrenbacher, L.; Novotny, W.; Cartwright, T.; Hainsworth, J.; Heim, W.; Berlin, J.; Baron, A.; Griffing, S.; Holmgren, E.; Ferrara, N.; Fyfe, G.; Rogers, B.; Ross, R.; Kabbinavar, F. Bevacizumab plus irinotecan, fluorouracil, and leucovorin for metastatic colorectal cancer. *N. Engl. J. Med.* **2004**, *350*, 2335–2342. (b) Sandler, A.; Gray, R.; Perry, M. C.; Brahmer, J.; Schiller, J. H.; Dowlati, A.; Lilenbaum, R.; Johnson, D. H. Paclitaxel−carboplatin alone or with bevacizumab for non-small-cell lung cancer. *N. Engl. J. Med.* **2006**, *355*, 2542–2550.

(11) Adjei, A. A. Novel small-molecule inhibitors of the vascular endothelial growth factor receptor. *Clin. Lung Cancer* **2007**, *8* (Suppl. 2), S74–S78.

(12) (a) Thomas, A. L.; Morgan, B.; Dreves, J.; Unger, C.; Wiedenmann, B.; Vanhoefer, U.; Laurent, D.; Dugan, M.; Steward, W. P. Vascular endothelial growth factor receptor tyrosine kinase inhibitors: PTK787/ZK 222584. *Semin. Oncol.* **2003**, *30* (Suppl. 6), 32–38. (b) Ryan, A. J.; Wedge, S. R. ZD6474, a novel inhibitor of VEGFR and EGFR tyrosine kinase activity. *Br. J. Cancer* **2005**, *92* (Suppl. 1), S6–S13. (c) Sun, L.; Liang, C.; Shirazian, S.; Zhou, Y.; Miller, T.; Cui, J.; Fukuda, J. Y.; Chu, J.-Y.; Nematalla, A.; Wang, X.; Chen, H.; Sistla, A.; Luu, T. C.; Tang, F.; Wei, J.; Tang, C. Discovery of 5-[5-fluoro-2-oxo-1,2- dihydroindol-(3*Z*)-ylidenemethyl]-2,4-dimethyl-1*H*-pyrrole-3-carboxylic acid (2-diethylaminoethyl)amide, a novel tyrosine kinase inhibitor targeting vascular endothelial and platelet-derived growth factor receptor tyrosine kinase. *J. Med. Chem.* **2003**, *46*, 1116–1119. (d) Gingrich, D. E.; Reddy, D. R.; Iqbal, M. A.; Singh, J.; Aimone, L. D.; Angeles, T. S.; Albom, M.; Yang, S.; Ator, M. A.; Meyer, S. L.; Robinson, C.; Ruggeri, B. A.; Dionne, C. A.; Vaught, J. L.; Mallamo, J. P.; Hudkins, R. L. A new class of potent vascular endothelial growth factor receptor tyrosine kinase inhibitors: structure activity relationships for a series of 9-alkoxymethyl-12-(3-hydroxypropyl)indeno[2,1-*a*]pyrrolo[3,4-*c*]carbazole-5-ones and the identification of CEP-5214 and its dimethylglycine ester prodrug clinical candidate CEP-7055. *J. Med. Chem.* **2003**, *46*, 5375–5388. (e) Hennequin, L. F.; Stokes, E. S. E.; Thomas, A. P.; Johnstone, C.; Ple, P. A.; Ogilvie, D. J.; Dukes, M.; Wedge, S. R.; Kendrew, J.; Curwen, J. O. Novel 4-anilinoquinazolines with C-7 basic side chains: design and structure activity relationship of a series of potent, orally active, VEGF receptor tyrosine kinase inhibitors. *J. Med. Chem.* **2002**, *45*, 1300–1312. (f) Ruggeri, B.; Singh, J.; Gingrich, D.; Angeles, T.; Albom, M.; Chang, H.; Robinson, C.; Hunter, K.; Dobrzanski, P.; Jones-Bolin, S.; Aimone, L.; Klein-Szanto, A.; Herbet, J.-M.; Bono, F.; Schaeffer, P.; Casellas, P.; Bourie, B.; Pili, R.; Isaacs, J.; Ator, M.; Hudkins, R.; Vaught, J.; Mallamo, J.; Dionne, C. CEP-7055: a novel, orally active pan inhibitor of vascular endothelial growth factor receptor tyrosine kinases with potent antiangiogenic activity and antitumor efficacy in preclinical models. *Cancer Res.* **2003**, *63*, 5978–5991. (g) Beebe, J. S.; Jani, J. P.; Knauth, E.; Goodwin, P.; Higdon, C.; Rossi, A. M.; Emerson, E.; Finkelstein, M.; Floyd, E.; Harriman, S.; Atherton, J.; Hillerman, S.; Soderstrom, C.; Kou, K.; Gant, T.; Noe, M. C.; Foster, B.; Rastinejad, F.; Marx, M. A.; Schaeffer, T.; Whalen, P. M.; Roberts, W. G. Pharmacological characterization of CP-547,632, a novel vascular endothelial growth factor receptor-2 tyrosine kinase inhibitor for cancer therapy. *Cancer Res.* **2003**, *63*, 7301–7309.

(13) (a) Mross, K.; Drevs, J.; Muller, M.; Medinger, M.; Marme, D.; Hennig, J.; Morgan, B.; Lebwohl, D.; Masson, E.; Ho, Y. Y.; Guenther, C.; Laurent, D.; Unger, C. Phase I clinical and pharmacokinetic study of PTK/ZK, a multiple VEGF receptor inhibitor, in patients with liver metastases from solid tumours. *Eur. J. Cancer* **2005**, *41*, 1291–1299. (b) Thomas, A. L.; Morgan, B.; Horsfield, M. A.; Higginson, A.; Kay, A.; Lee, L.; Masson, E.; Puccio-Pick, M.; Laurent, D.; Steward, W. P. Phase I study of the safety, tolerability, pharmacokinetics, and pharmacodynamics of PTK787/ZK 222584 administered twice daily in patients with advanced cancer. *J. Clin. Oncol.* **2005**, *23*, 4162–4171.

(14) Rini, B. I. Sorafenib. *Expert Opin. Pharmacother.* **2006**, *7*, 453–461.

(15) (a) Atkins, M.; Jones, C. A.; Kirkpatrick, P. Sunitinib maleate. *Nat. Rev. Drug Discovery* **2006**, *5*, 279–280. (b) Fiedler, W.; Serve, H.; Doehner, H.; Schwittay, M.; Ottmann, O. G.; O'Farrell, A. M.; Bello, C. L.; Allred, R.; Manning, W. C.; Cherrington, J. M.; Louie, S. G.; Hong, W.; Brega, N. M.; Massimini, G.; Scigalla, P.; Berdel, W. E.; Hossfeld, D. K. A phase 1 study of SU11248 in the treatment of patients with refractory or resistant acute myeloid leukemia (AML) or not amenable to conventional therapy for the disease. *Blood* **2005**, *105* (3), 986–993.

(16) Polverino, A.; Coxon, A.; Starnes, C.; Diaz, Z.; DeMelfi, T.; Wang, L.; Bready, J.; Estrada, J.; Cattley, R.; Kaufman, S.; Chen, D.; Gan, Y.; Kumar, G.; Meyer, J.; Neervannan, S.; Alva, G.; Talvenheimo, J.; Montestruque, S.; Tasker, A.; Patel, V.; Radinsky, R.; Kendall, R. AMG 706, an oral, multikinase inhibitor that selectively targets vascular endothelial growth factor, platelet-derived growth factor, and Kit receptors, potently inhibits angiogenesis and induces regression in tumor xenografts. *Cancer Res.* **2006**, *66*, 8715–8721.

(17) *Daylight*, version 4.41; Daylight Chemical Information Systems, Inc.: Irvine, CA, 1995.

(18) Harmange, J.-C.; Weiss, M. M.; Germain, J.; Polverino, A. J.; Borg, G.; Bready, J.; Chen, D.; Choquette, D.; Coxon, A.; DeMelfi, T.; DiPietro, L.; Doerr, N.; Estrada, J.; Flynn, J.; Graceffa, R. F.; Harriman, S. P.; Kaufman, S.; La, D. S.; Long, A.; Martin, M. W.; Neervannan, S.; Patel, V. F.; Potashman, M.; Regal, K.; Roveto, P. M.; Schrag, M. L.; Starnes, C.; Tasker, A.; Teffera, Y.; Wang, L.; White, R. D.; Whittington, D.; Zanon, R. Naphthamides as novel and potent vascular endothelial growth factor receptor tyrosine kinase inhibitors: design, synthesis, and evaluation. *J. Med. Chem.* **2008**, *51*, 1649–1667.

(19) Nigg, E. A. Mitotic kinases as regulators of cell division and its checkpoints. *Nat. Rev. Mol. Cell Biol.* **2001**, *2*, 21–32.

(20) Palacios, E. H.; Weiss, A. Function of the Src-family kinases, Lck and Fyn, in T-cell development and activation. *Oncogene* **2004**, *23*, 7990–8000.

(21) (a) He, M.; Kania, R. S.; Lou, J.; Zhou, R. Preparation of Naphthalenecarboxamides and Their Derivatives as New Antiangiogenic Agents. WO 2005/021553 A1, 2005. (b) Potashman, M.; Kim, T.; Bellon, S.; Booker, S.; Cheng, Y.; Kim, J. L.; Tasker, A.; Xi, N.; Xu, S.; Harmange, J.-C.; Borg, G.; Weiss, M.; Hodous, B. L.; Graceffa, R.; Buckner, W. H.; Masse, C. E.; Choquette, D.; Martin, M. W.; Germain, J.; Dipietro, L. V.; Chaffee, S. C.; Nunes, J. J.; Buchanan, J. L.; Habgood, G. J.; McGowan, D. C.; Whittington, D. A. Preparation of Heteroaryl Substituted Naphthalenes as Inhibitors of Lck, VEGFR and/or HGF Related Activity. WO 2005/070891 A2, 2005.

(22) De, D.; Krogstad, F. M.; Byers, L. D.; Krogstad, D. J. Structure−activity relationships for antiplasmodial activity among 7-substituted 4-aminoquinolines. *J. Med. Chem.* **1998**, *41*, 4918–4926.

(23) Lindley, J. Copper assisted nucleophilic substitution of aryl halogen. *Tetrahedron* **1984**, *40*, 1433–1456.

(24) Nomoto, Y.; Obase, H.; Takai, H.; Hirata, T.; Teranishi, M.; Nakamura, J.; Kubo, K. Studies on cardiotonic agents. I. Synthesis of some quinazoline derivatives. *Chem. Pharm. Bull.* **1990**, *38*, 1591–1595.

(25) Tan, H.; Semin, D.; Wacker, M.; Cheetham, J. An automated screening assay for determination of aqueous equilibrium solubility enabling SPR study during drug lead optimization. *J. Assoc. Lab. Autom.* **2005**, *10* (6), 364–373.

(26) (a) Shaffer, C. L.; Morton, M. D.; Hanzlik, R. P. Enzymatic N-dealkylation of an *N*-cyclopropylamine: an unusual fate for the cyclopropyl group. *J. Am. Chem. Soc.* **2001**, *123*, 349–350. (b) Kalgutkar, A. S.; Gardner, I.; Obach, R. S.; Shaffer, C. L.; Callegari, E.; Henne, K. R.; Mutlib, A. E.; Dalvie, D. K.; Lee, J. S.; Nakai, Y.; O'Donnell, J. P.; Boer, J.; Harriman, S. P. A comprehensive listing of bioactivation pathways of organic functional groups. *Curr. Drug. Metab.* **2005**, *6*, 161–225.

(27) Evans, D. C.; Watt, A. P.; Nicoll-Griffith, D. A.; Baillie, T. A. Drug−protein adducts: an industry perspective on minimizing the potential for drug bioactivation in drug discovery and development. *Chem. Res. Toxicol.* **2004**, *17*, 3–16.
(28) Radiolabeled compounds were prepared wherein the carbon of amide carbonyl was labeled with ^{14}C.
(29) Obach, R. S. Prediction of human clearance of twenty-nine drugs from hepatic microsomal intrinsic clearance data: an examination of in vitro half-life approach and nonspecific binding to microsomes. *Drug Metab. Dispos.* **1999**, *27*, 1350–1359.
(30) Miles, A. A.; Miles, E. M. Vascular reactions to histamine, histamine-liberator,and leukotaxine in the skin of guinea pigs. *J. Physiol.* **1952**, *118*, 228–257.
(31) Coxon, A.; Bolon, B.; Estrada, J.; Kaufman, S.; Scully, S.; Rattan, A.; Duryea, D.; Hu, Y. L.; Rex, K.; Pacheco, E.; Van, G.; Zack, D.; Feige, U. Inhibition of interleukin-1 but not tumor necrosis factor suppresses neovascularization in rat models of corneal angiogenesis and adjuvant arthritis. *Arthritis Rheum.* **2002**, *46*, 2604–2612.

JM701098W